Additional files provided with this submission:

Additional file 1: 1707034934143172_add1.doc, 154K
http://www.biomedcentral.com/imedia/1250732549153883/supp1.doc

J Physiol Sci (2015) 65:121–130
DOI 10.1007/s12576-014-0349-0

ORIGINAL PAPER

A comparison of chronic AICAR treatment-induced metabolic adaptations in red and white muscles of rats

Masataka Suwa · Hiroshi Nakano · Zsolt Radak · Shuzo Kumagai

Received: 26 March 2014 / Accepted: 30 October 2014 / Published online: 12 November 2014

Abstract The signaling molecule 5′-AMP-activated protein kinase plays a pivotal role in metabolic adaptations. Treatment with 5-aminoimidazole-4-carboxamide-1-β-D-ribofranoside (AICAR) promotes the expression of metabolic regulators and components involved in glucose uptake, mitochondrial biogenesis, and fatty acid oxidation in skeletal muscle cells. Our aim was to determine whether AICAR-induced changes in metabolic regulators and components were more prominent in white or red muscle. Rats were treated with AICAR (1 mg/g body weight/day) for 14 days, resulting in increased expression levels of nicotinamide phosphoribosyltransferase (NAMPT), peroxisome proliferator-activated receptor-γ coactivator-1α (PGC-1α), glucose transporter 4 proteins, and enhanced mitochondrial biogenesis. These changes were more prominent in white rather than red gastrocnemius muscle or were only observed in the white gastrocnemius. Our results suggest that AICAR induces the expression of metabolic regulators and components, especially in type II (B) fibers.

Keywords AMP-activated protein kinase · Mitochondrial biogenesis · Nicotinamide phosphoribosyltransferase · SIRT1 · Skeletal muscle

M. Suwa (✉)
Faculty of Life Design, Tohoku Institute of Technology, 6 Futatsusawa, Taihaku-ku, Sendai, Miyagi 982-8588, Japan
e-mail: suwa-m@tohtech.ac.jp

H. Nakano
Faculty of Education, Nakamura Gakuen University, Jonan-ku, Fukuoka 814-0198, Japan

Z. Radak
Institute of Sport Science, Faculty of Physical Education and Sport Science, Semmelweis University, Budapest, Hungary

S. Kumagai
Faculty of Arts and Science, Kyushu University, Kasuga, Fukuoka 816-8580, Japan

S. Kumagai
Graduate School of Human-Environment Studies, Kyushu University, Kasuga, Fukuoka 816-8580, Japan

Introduction

Skeletal muscle demonstrates a great degree of metabolic plasticity, with its characteristics subjected to many studies over several decades. Accumulating evidence suggests that a large number of signaling molecules control the metabolic properties of skeletal muscle. The signaling molecule 5′-AMP-activated protein kinase (AMPK) has been shown to play a pivotal role in skeletal muscle cells [1].

AMPK is a heterotrimer comprising catalytic α- and regulatory β- and γ-subunits [2]. Two isoforms exist for the α-subunit (α1 and α2) and the β-subunit (β1 and β2), with three isoforms for the γ-subunit (γ1, γ2, and γ3). The α-subunit contains the serine/threonine kinase domain, which has been shown to exhibit kinase activity when it is phosphorylated by upstream kinases such as LKB1 and CaMKK [3, 4]. The β-subunit contains a domain that interacts with the α- and γ-subunits and was previously reported to mediate the assembly of the heterotrimeric AMPK complex [5]. The β-subunit also contains a glycogen-binding domain [6]. The γ-subunit binds to AMP following the phosphorylation of threonine 172 in the α-subunit and kinase activation [7]. AMPK is a central energy-sensing master regulator of cellular metabolism and is activated when the cellular AMP/ATP ratio increases [8]. This allosteric regulatory system further promotes the

phosphorylation of threonine 172 in the α-subunit by upstream kinases [9].

Skeletal muscle AMPK is known to be activated by exercise [10, 11]; secretory factors including leptin [12], adiponectin [13], interleukin-6 [14], and brain-derived neurotrophic factor [15]; and antidiabetic drugs [16, 17]. It is also activated by the adenosine analog 5-aminoimidazole-4-carboxamide-1-β-D-ribofranoside (AICAR); AICAR activation of AMPK stimulates glucose uptake and fatty acid oxidation in skeletal muscle cells [18]. AICAR treatment has also been found to enhance the expression of metabolic components, including glucose transporter 4 (GLUT4) and monocarboxylate transporters 1 and 4 proteins; increase hexokinase activity; and stimulate mitochondrial biogenesis in skeletal muscle [19–22]. Activation of AMPK has been linked to upregulated expression of metabolic regulators, such as silent information regulator of transcription 1 (SIRT1), peroxisome proliferator-activated receptor (PPAR)-γ coactivator-1α (PGC-1α), and nicotinamide phosphoribosyltransferase (NAMPT) [21, 23, 24]. It has been proposed that AMPK-induced metabolic adaptations could be mediated, at least partially, by SIRT1 [1].

SIRT1 is an oxidized form of nicotinamide adenine dinucleotide (NAD^+)-dependent histone deacetylase. It plays an important role in various biological processes via its interactions with and deacetylation of many transcriptional regulators, such as forkhead transcription factor (FOXO) [25], p53 [26], nuclear factor-κB (NF-κB) [27], and PGC-1α [28]. SIRT1 regulates mitochondrial biogenesis and fatty acid oxidation in skeletal muscle cells by deacetylating and functionally activating PGC-1α [28, 29].

SIRT1 activity is controlled by NAMPT, also known as pre-B cell colony-enhancing factor (PBEF) or visfatin. NAMPT is the rate-limiting enzyme required for the synthesis of NAD^+ from nicotinamide, an inhibitor of SIRT1. NAMPT increases the NAD^+/NADH ratio and decreases nicotinamide concentrations: SIRT1 activity then allosterically increases in skeletal muscle cells [30]. The metabolic capacity of skeletal muscle is thought to be at least partially controlled by the AMPK–NAMPT–SIRT1–PGC-1α axis. The expression of NAMPT in skeletal muscle has been shown to increase with endurance exercise training and activation of AMPK [23, 31, 32]. NAMPT might play an important role in exercise training-induced metabolic adaptations in skeletal muscle [33].

Skeletal muscle fibers in rodents are categorized as slow-twitch type I and fast-twitch type IIA, IIX and IIB fibers, and express myosin heavy chains I, IIA, IIX, and IIB, respectively [34]. The type I, IIA, and IIX fibers exist in human skeletal muscle [34]. The rank order of maximum contraction velocity in rat skeletal muscle fibers is I < IIA < IIX < IIB [35]; for oxidative capacity it is IIB < I < IIX < IIA [36] or IIB < IIX < I < IIA [37]. Metabolic responses to some stimuli, such as exercise training [38], detraining [39], and hindlimb suspension [40], appear to differ among the various fiber types. Acute exercise was reported to increase the AMPK phosphorylation in all fiber types, and type IIX fibers exhibited the greatest increase in human skeletal muscle [41].

We previously showed that AICAR induces increases in AMPK phosphorylation levels in type II fiber-rich extensor digitorum longus (EDL) muscle. The extent of this increase appeared to be greater than that in the type I fiber-rich soleus muscle of rats [24]. In another study, it was shown that a single AICAR injection resulted in a 5.5-fold increase in AMPK activity in the white gastrocnemius muscle, but only a 2.9-fold increase in the red gastrocnemius muscle [42]. Collectively, these findings suggested that acute administration of AICAR increases phosphorylation levels of AMPK in type II(B) fibers to a great extent than in type I fibers. Therefore, chronic AICAR treatment might result in greater expression levels of metabolic regulators and components in type II(B) fiber-rich white muscle compared with those in type I fiber-rich red muscles. However, results from previous studies have not clearly revealed the extent of chronic AICAR treatment-induced metabolic adaptations between muscles types. We hypothesized that chronic AICAR treatment would enhance expression levels of metabolic regulators and components. We also believe that these effects would be more prominent in type II(B) fibers than in type I fibers.

Our aims were to determine whether AICAR-induced changes in metabolic regulators, such as NAMPT, SIRT1, and PGC-1α, and in metabolic components, such as GLUT4 and mitochondrial oxidative enzymes, differed between type I fiber-rich red gastrocnemius and type IIB fiber-rich white gastrocnemius muscles.

Materials and methods

Animal studies

Male Wistar rats (5 weeks old, 136–148 g) from Kyudo (Tosu, Saga, Japan) were used in this study. All rats were handled daily for at least 5 days before the commencement of experiments. Rats were housed in a temperature-(22 ± 2 °C) and humidity-controlled (60 ± 5 %) room with a 12-h light (07:00–19:00):12-h dark (19:00–07:00) cycle; food and water were provided ad libitum. All experimental procedures were strictly conducted in accordance with the Nakamura Gakuen University guidelines for the Care and Use of Laboratory Animals and were approved by the University Animal Experiment Committee.

Rats were divided into control ($n = 9$) and AICAR treatment ($n = 7$) groups. Rats in the control group were given daily subcutaneous injections of saline, while those in the AICAR group were given daily subcutaneous injections of AICAR (1 mg/g body weight; Toronto Research Chemicals, North York, ON, Canada). This dose of AICAR was previously shown to enhance skeletal muscle AMPK activity and the phosphorylation of threonine 172 in the α-subunit at 60 and 120 min postinjection [19, 24, 43, 44]. Procedures were performed between 08:00 and 10:00 for 14 successive days. Nonfasted rats were intraperitoneally anesthetized with pentobarbital sodium (60 mg/kg body weight) about 24 h after the last injection. The gastrocnemius muscle was dissected, and the deep (red) and superficial (white) portions of the lateral head of the gastrocnemius muscle were isolated. Muscle tissues were immediately frozen in liquid nitrogen and stored at −80 °C until required. The abdominal fat pads (mesenteric, epididymal and perirenal) were also excised and weighed.

Preparation of muscle samples

Frozen muscle samples were homogenized in ice-cold homogenization buffer (1:10 w/v; 25 mM HEPES, 250 mM sucrose, 2 mM EDTA, 0.1 % Triton X-100, pH 7.4) supplemented with Complete™ Protease Inhibitor Cocktail Tablets (Roche Diagnostics, Tokyo, Japan) and centrifuged (15,000×*g*, 4 °C, 25 min). The supernatant was removed and the concentration of proteins determined using a kit (Bio-Rad, Richmond, CA). This muscle homogenate was used for enzymatic assays and in Western blotting analyses. For the Western blotting analyses, the muscle protein homogenate was solubilized in sample loading buffer (50 mM Tris-HCl pH 6.8, 2 % sodium dodecyl sulfate, 10 % glycerol, 5 % β-mercaptoethanol, and 0.005 % bromophenol blue).

Western blotting

Proteins (20 μg) present in homogenates were separated by sodium-dodecylsulfate-polyacrylamide gel electrophoresis (SDS-PAGE) using 7.5 % (SIRT1 and PGC-1α), 10 % (NAMPT and GLUT4), and 15 % (cytochrome C) resolving gels. Proteins separated by SDS-PAGE were electrophoretically transferred to polyvinylidene difluoride membranes. These membranes were incubated with a blocking buffer of casein solution (Vector Laboratories, Burlingame, CA, USA) for 1 h at room temperature. Membranes were incubated with rabbit polyclonal antibodies against PBEF (1:500 dilution; Bethyl Laboratories, Inc., Montgomery, TX, USA), Sir2 (1:1000; Upstate Biotechnology, Lake Placid, NY, USA), PGC-1α (1:500; AB3242, Chemicon International, Temecula, CA, USA), or GLUT4 (1:8000; Chemicon International), or with a mouse monoclonal antibody against cytochrome C (1:200; clone 7H8.2C12; Biosource, Camarillo, CA, USA) overnight at 4 °C. Membranes were then incubated with anti-rabbit/mouse biotinylated IgG (1:1000; Vector Laboratories) for 30 min. Protein bands were visualized using the avidin and biotinylated horseradish peroxidase macromolecular complex technique (Vector Laboratories). Band densities were determined using NIH Image, version 1.62 (National Institute of Health, Bethesda, MD, USA).

Enzyme activity assays

Enzyme activities were measured spectrophotometrically with assays conducted at 30 °C using saturating concentrations of substrates and cofactors, as previously determined. Citrate synthase (CS) activity was measured at 412 nm to detect the transfer of sulfhydryl groups to 5, 5′-dithiobis(2-nitrobenzonic acid) (DTNB). The extinction coefficient for DTNB was 13.6. Hexokinase (HK), pyruvate kinase (PK), lactate dehydrogenase (LDH), malate dehydrogenase (MDH), and β-hydroxyacyl-coenzyme A dehydrogenase (βHAD) activities were measured at 340 nm by following the production or consumption of NADH or NADPH over 3 min. The extinction coefficient for NAD(P)H was 6.22. Further details and procedures have been described previously [45].

Statistical analysis

Values are expressed as the mean ± SD. We used the unpaired *t* test to compare data between groups with a *P* value less than 0.05 considered statistically significant.

Results

Body composition

We summarized the body composition of rats (Table 1); pre- and posttreatment body masses in the AICAR group were not significantly different from those in the control

Table 1 Body composition of rats in the current study

	Control ($n = 9$)	AICAR ($n = 7$)
Pretreatment body weight (g)	140 ± 3	141 ± 3
Posttreatment body weight (g)	245 ± 13	238 ± 8
Mesenteric fat tissue weight (g)	3.19 ± 0.41	2.44 ± 0.52*
Epididymal fat tissue weight (g)	1.81 ± 0.16	1.32 ± 0.14*
Perirenal fat tissue weight (g)	0.39 ± 0.06	0.23 ± 0.07*

* $P < 0.05$ vs. control group

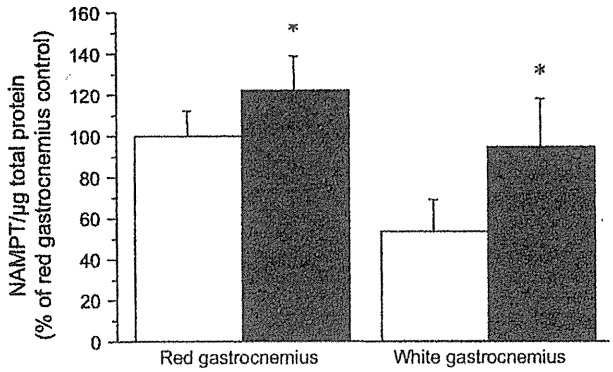

Fig. 1 NAMPT protein expression levels in red and white gastrocnemius muscles of rats in the control (*open columns*) and AICAR (*filled columns*) groups. Values are mean ± SD; $n = 7$–9 muscles per group. $^*P < 0.05$ *vs.* the control group

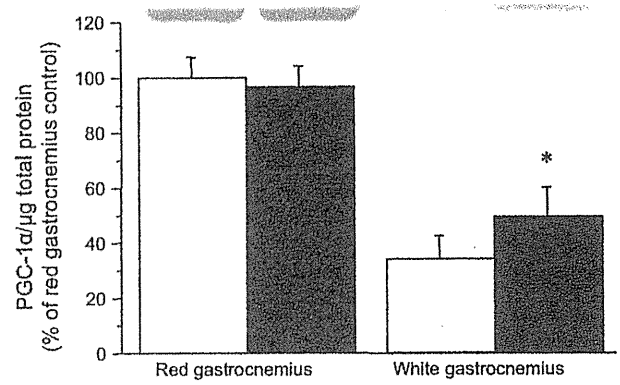

Fig. 3 PGC-1α protein expression levels in red and white gastrocnemius muscles of rats in the control (*open columns*) and AICAR (*filled columns*) groups. Values are mean ± SD; $n = 7$–9 muscles per group. $^*P < 0.05$ *vs.* the control group

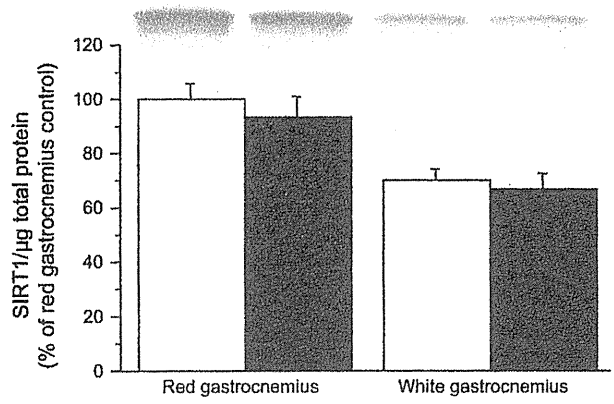

Fig. 2 SIRT1 protein expression levels in red and white gastrocnemius muscles of rats in the control (*open columns*) and AICAR (*filled columns*) groups. Values are mean ± SD; $n = 7$–9 muscles per group

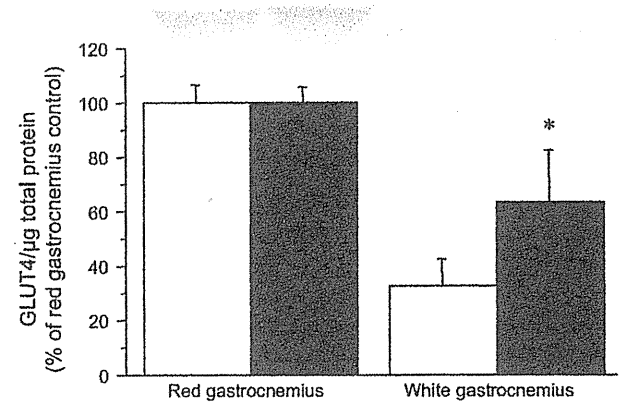

Fig. 4 GLUT4 protein expression levels in red and white gastrocnemius muscles of rats in the control (*open columns*) and AICAR (*filled columns*) groups. Values are mean ± SD; $n = 7$–9 muscles per group. $^*P < 0.05$ *vs.* the control group

group. Mesenteric, epididymal, and perirenal fat tissue masses in the AICAR group were significantly lower than those in the control group.

Expression of metabolic regulators

NAMPT protein expression levels in red and white gastrocnemius muscles were significantly increased, by 22 and 77 %, respectively ($P < 0.01$), following AICAR treatment (Fig. 1). SIRT1 protein expression levels were unaltered by AICAR treatment in red or white muscles (Fig. 2). PGC-1α protein expression levels in the white gastrocnemius muscle of rats in the AICAR group were significantly higher than those in the control group (47 %, $P < 0.01$); however, a similar difference was not observed in red gastrocnemius muscle (Fig. 3).

Expression of metabolic components

AICAR treatment significantly increased GLUT4 protein expression levels by 96 % in white gastrocnemius muscle ($P < 0.001$), but not in red gastrocnemius muscle (Fig. 4). Cytochrome C protein expression levels in the white gastrocnemius muscle were also increased by the AICAR treatment (26 %, $P < 0.05$). We did not observe any changes in cytochrome C expression levels in red gastrocnemius muscle (Fig. 5).

Enzyme activities

HK activities in red and white gastrocnemius muscles were significantly increased in the AICAR-treated group, by 52 and 132 %, respectively, compared to the control group

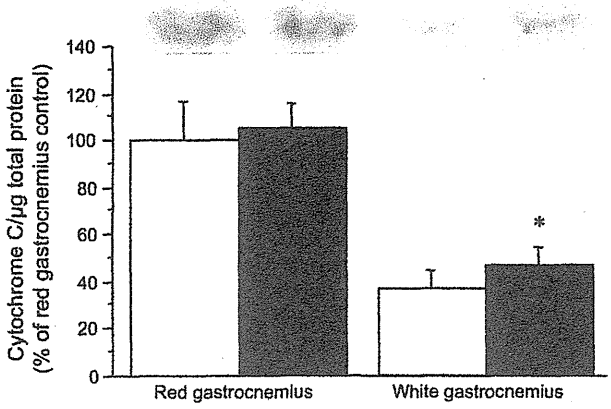

Fig. 5 Cytochrome C protein expression levels in red and white gastrocnemius muscle of rats in the control (*open columns*) and AICAR (*filled columns*) groups. Values are mean ± SD; $n = 7$–9 muscles per group. *$P < 0.05$ *vs.* the control group

(Fig. 6a; $P < 0.0001$). PK activity in white gastrocnemius muscle was increased by 26 % because of AICAR treatment ($P < 0.0001$); however, PK activity was relatively unchanged in red gastrocnemius muscle (Fig. 6b). AICAR treatment did not affect LDH activity in either type of muscle (Fig. 6c). CS activity in white gastrocnemius muscle was significantly higher in the AICAR-treated group compared with that in the control group (26 %, $P < 0.0001$). No significant differences were observed for CS activity in red gastrocnemius muscle (Fig. 6d). MDH activities in red and white gastrocnemius muscles were significantly increased by 13 and 38 %, respectively, following AICAR treatment ($P < 0.05$; Fig. 6e) compared with those seen in the control group. AICAR treatment resulted in a 31 % increase in βHAD activity in white gastrocnemius muscle ($P < 0.01$), with no increase observed in red gastrocnemius muscle (Fig. 6f).

Comparison of AICAR effects in red and white muscles

We have illustrated the relative changes in protein expression levels and metabolic enzyme activities induced by AICAR treatment and compared them with those in the control group (Fig. 7). AICAR induced changes for all parameters relative to the control group, with the exception of SIRT1 protein and LDH activity levels. These were significantly higher in white gastrocnemius muscle compared with that in red gastrocnemius muscle ($P < 0.05$).

Discussion

AMPK has been implicated in several diseases such as diabetes mellitus, hypertension, cardiac hypertrophy, cancer, dementia, and stroke [46]. The control of AMPK activity represents a strategy for preventing these diseases or improving therapies against them. In our current study, we found that treating rats with AICAR over 14 successive days significantly increased expression levels of NAMPT, PGC-1α, and GLUT4 proteins and enhanced mitochondrial biogenesis in rat skeletal muscle.

We designed our study so as to compare AICAR-induced metabolic alterations in red and white muscles.

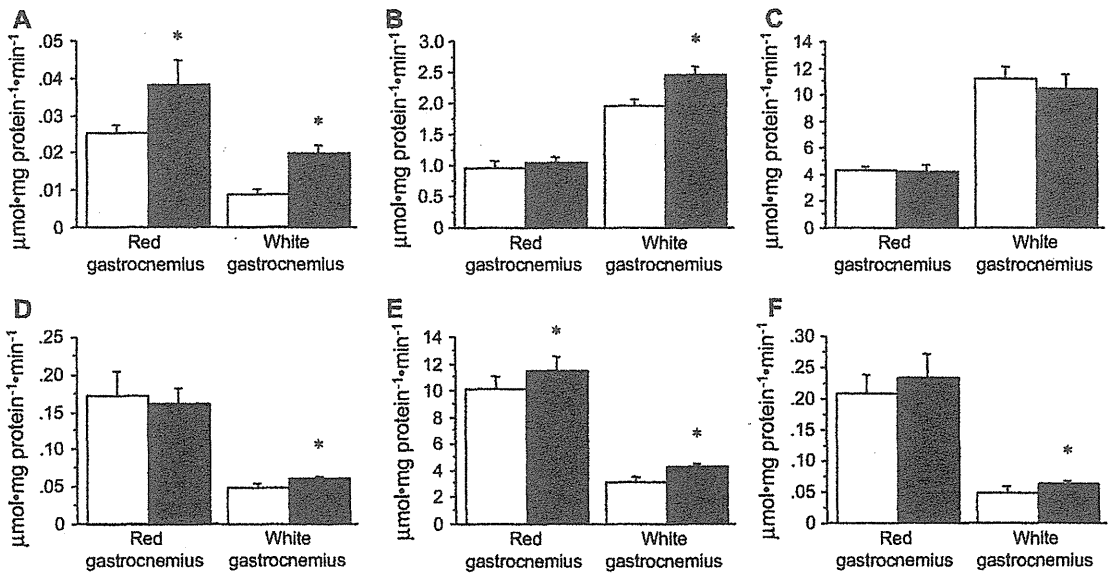

Fig. 6 Metabolic enzyme activities in red and white gastrocnemius muscles. **a** Hexokinase, **b** pyruvate kinase, **c** lactate dehbydrogenase, **d** citrate synthase, **e** malate dehydrogenase, and **f** β-hydroxyacyl-coenzyme A dehydrogenase in rats of the control (*open columns*) and AICAR (*filled columns*) groups. Values are mean ± SD; $n = 7$–9 muscles per group. *$P < 0.05$ *vs.* the control group

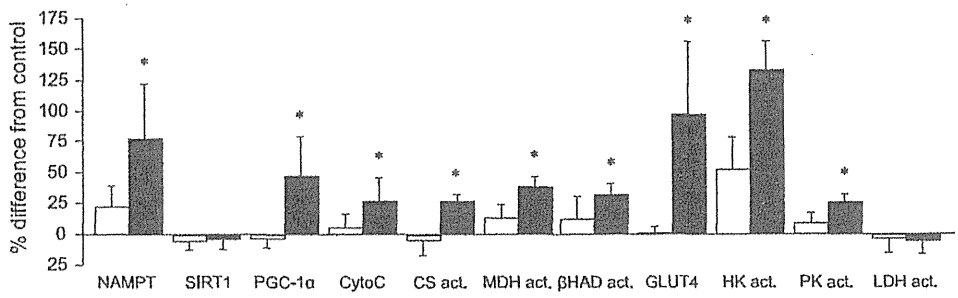

Fig. 7 Proportional differences in protein expression levels and metabolic enzyme activity levels between rats in the control and AICAR groups for red (*open columns*) and white (*filled columns*) gastrocnemius muscles. Differences in these measurements were determined as follows: % difference = 100 × (AICAR group/mean control group) − 100. Values are mean ± SD; $n = 7$ per group. *$P < 0.05$ *vs.* red gastrocnemius muscle. *CytoC* cytochrome C, *act.* activity

Our results showed that the expression levels of metabolic regulators, such as NAMPT and PGC-1α proteins, following the AICAR treatment were higher in the white gastrocnemius muscle than in the red gastrocnemius muscle. Furthermore, the expression of the GLUT4 and cytochrome C proteins as well as CS, MDH, βHAD, HK, and PK activities were higher in the white gastrocnemius muscle than in the red gastrocnemius muscle following the AICAR treatment. The red gastrocnemius muscle contains ~50 % type I fibers and less than 1 % type IIB fibers. The white gastrocnemius muscle contains ~90 % type IIB and ~10 % of type IIX fibers, with low levels but a minimal amount of type I or IIA fibers in rats [37, 47]. Based on these results, AICAR-induced metabolic improvements were suggested to be more prominent in type II(B) fibers than in type I fibers.

The fiber type-dependent effects of AICAR on muscle metabolic profiles observed in our present study could be partially associated with different AMPK phosphorylation levels among fiber types following AICAR treatment. We previously showed that acute AICAR treatment-induced increases in AMPK phosphorylation levels appeared to be greater in type II fiber-rich EDL muscle than in type I fiber-rich soleus muscle [24]. Additionally, phosphorylation levels of acetyl-coenzyme A carboxylase (ACC), a downstream target of AMPK, in the EDL muscle appeared to be enhanced to a great extent than in the soleus muscle following AICAR treatment [24]. Previous results indicate that a single AICAR injection resulted in a 5.5-fold increase in AMPK activity in white gastrocnemius muscle, but only a 2.9-fold increase in red gastrocnemius muscle [42]. These fiber type-dependent effects of AICAR on the phosphorylation of AMPK might be responsible for the different results we observed in red and white muscles.

Another possible cause of these differences could be the varying expression patterns of the AMPK γ subunit isoforms among fiber types. In rodents, the AMPK γ3 isoform is primarily expressed in muscles that are rich in type IIB fibers, but is rarely expressed in type I fiber-rich muscles [48, 49]. The skeletal muscles of AMPK γ3 mutant (R225Q) transgenic mice exhibit enhanced mitochondrial biogenesis, fatty acid oxidation, and glycogen synthesis as well as increased expression levels of genes encoding the corresponding regulatory proteins [48, 50, 51]. In contrast, AMPK γ3 isoform knockout mice have decreased gene expression levels [50]. Cantó et al. [52] reported that fasting-induced increases in the expression of NAMPT, PGC-1α, and GLUT4 mRNA and exercise-induced increases in NAMPT mRNA expression and PGC-1α deacetylation were ameliorated in AMPK γ3 knockout mice. Incubating EDL muscle isolated from wild-type mice with AICAR promoted the phosphorylation of the AMPK downstream targets, such as ACC and the Akt substrate of 160 kDa (AS160); however, these changes were ablated in EDL muscles isolated from AMPK γ3 isoform knockout mice [53]. The AMPK γ3 isoform appears to be necessary for AICAR-induced AMPK signaling in skeletal muscle and controls AICAR-stimulated metabolic adaptations, especially in type IIB fibers.

Consistent with our results, AICAR treatment for 28 successive days was previously shown to increase NAMPT protein and mRNA expression levels in the skeletal muscle of mice [23]. The effects of AICAR on the accumulation of the NAMPT protein were not apparent in AMPK α2 kinase dead (nonfunctional enzyme) mice, whereas NAMPT mRNA levels were maintained [23]. The AICAR-induced increases observed in the expression of the NAMPT protein we observed can be attributed to regulation by AMPK signaling at the posttranscriptional or translational level. Results from a previous study demonstrated that AMPK controlled intracellular NAD^+ concentrations and SIRT1 activity [54]. Collectively, these results suggest that AMPK regulates SIRT1 activity by modulating the quantity of the NAMPT protein, followed by PGC-1α deacetylation and transcriptional activation.

The activated form of PGC-1α can interact with several transcription factors, including myocyte enhancer factor 2 (MEF2), GLUT4 enhancer factor (GEF), cAMP response

element binding protein (CREB), estrogen-related receptor α (ERRα), PPARα and γ, and nuclear respiratory factor 1 (NRF1). NRF promotes the expression of GLUT4 and PGC-1α, and also promotes mitochondrial biogenesis [1]. The AMPK-NAMPT-SIRT1-PGC-1α axis possibly mediates the AICAR-induced metabolic improvements we observed in skeletal muscle.

In a previous study, it was reported that SIRT1 protein expression levels were increased in EDL muscle following administration of a single dose of AICAR to rats [24]. In humans, one short period of intense activity promotes the phosphorylation of AMPKα and SIRT1 protein expression in the vastus lateralis muscle. The same level of activity with glucose ingestion did not lead to an increase in either AMPK phosphorylation or SIRT1 protein content [55]. Based of these findings, it appears likely that AMPK signaling regulates the SIRT1 protein content in skeletal muscle.

We demonstrated that 14 successive days of AICAR treatment did not alter the expression of SIRT1 in either red or white gastrocnemius muscle in rats. Chronic administration of AICAR (30 days) to *mdx* mice also failed to enhance the expression of SIRT1 mRNA [56]. Furthermore, 5 days of a successive AICAR treatment decreased SIRT1 protein expression levels in rats [57]. These findings suggest that the effects of AICAR treatment on SIRT1 expression in skeletal muscle in vivo differed depending on duration of the treatment period. Although administration of a single dose of AICAR was shown to promote AMPK activity [22, 24], long-term (28 days) AICAR treatment abolished the activation of AMPK in rat skeletal muscle [22, 58]. These results indicate treatment period-specific effects of AICAR that lead to the activation of AMPK and inconsistent SIRT1 expression patterns.

Another possibility is that chronic AICAR administration results in an excess of nutrients in skeletal muscle fibers. These are manifested as elevated glycogen stores and inhibit accumulation of the SIRT1 protein, thus masking the effects of AICAR. Caloric restriction was previously reported to increase SIRT1 protein expression levels in skeletal muscle [59], suggesting that the expression of the SIRT1 protein is inversely associated with energy stores. The concentration of glycogen at 22–25 h after a final AICAR injection in the skeletal muscle of rats treated with AICAR over 4 weeks was higher than that in saline-treated rats [22]. This finding suggests that long-term administration of AICAR results in constantly elevated glycogen concentrations in skeletal muscle that might interfere with accumulation of SIRT1. Further investigations are required to elucidate the mechanism(s) responsible for varying different results obtained between short- and long-term AICAR treatments with respect to SIRT1 expression.

Although AICAR stimulates skeletal muscle metabolism via the direct activation of AMPK [60], other indirect mechanisms might also mediate metabolic adaptations. As an example, AICAR can activate other AMP-sensing enzymes [61, 62]. AICAR also controls the secretion or production of hormones/cytokines that regulate metabolism, including insulin [63], adiponectin [64], interleukin 6 (IL-6) [65], and tumor necrosis factor-α (TNF-α) [64]. Adiponectin and IL-6 are activators of AMPK [13, 14], whereas TNF-α is an inhibitor of AMPK [66, 67]. Therefore, in vivo AICAR treatment-induced metabolic modifications in skeletal muscle could be attributed to the direct and indirect activation of AMPK and AMPK-independent mechanisms. The administration of AICAR to mice overexpressing α2 kinase-dead AMPK led to an increase in the expression of NAMPT mRNA but not the corresponding protein [23], suggesting that AICAR affects the expression of NAMPT at the transcriptional level via an AMPK-independent mechanism.

In this study, we demonstrated that chronic AICAR treatment significantly decreased the mass of abdominal fat pads with concomitant increases in the expression of metabolic regulator proteins and mitochondrial components. Although the reasons for such reductions currently remain unclear, it is possible that increases in fatty acid oxidation and oxidative capacity in skeletal muscle induced by AICAR enhanced whole-body energy expenditure. Alternatively, it is possible that treatment with AICAR results in a slightly reduced food intake. However, slight caloric restriction should not affect metabolic modifications caused by AICAR. We previously demonstrated that caloric restriction of around 65 % in ad libitum-fed rats for 14 days did not affect expression of metabolic regulator proteins or mitochondrial components in skeletal muscle [45].

In conclusion, chronic AICAR treatment of rats for 14 successive days significantly increased NAMPT and PGC-1α protein expression levels in red and white gastrocnemius muscles. GLUT4 protein expression levels were also increased, and mitochondrial biogenesis was enhanced in skeletal muscles following AICAR treatment. These increases in the expression of metabolic regulators and components in white gastrocnemius muscle were more prominent than those in red gastrocnemius muscle, suggesting that AICAR-induced metabolic adaptations occurred, particulaly in type II(B) fibers. In contrast, long-term administration of AICAR did not affect SIRT1 expression.

Acknowledgments This work was supported by a Grant-in-Aid for Young Scientists from the Ministry of Education, Culture, Sports, Science, and Technology of Japan (no. 20700524) to MS.

Conflict of interest We have no conflicts of interest to declare.

References

1. Suwa M (2013) AMPK: molecular mechanisms of metabolic adaptations in skeletal muscle. In: Sakuma K (ed) Basic biology and current understanding of skeletal muscle. Nova Science Publishers Inc, New York
2. Winder WW (2001) Energy-sensing and signaling by AMP-activated protein kinase in skeletal muscle. J Appl Physiol 91:1017–1028
3. Sakamoto K, McCarthy A, Smith D, Green KA, Grahame Hardie D, Ashworth A, Alessi DR (2005) Deficiency of LKB1 in skeletal muscle prevents AMPK activation and glucose uptake during contraction. EMBO J 24:1810–1820
4. Hawley SA, Pan DA, Mustard KJ, Ross L, Bain J, Edelman AM, Frenguelli BG, Hardie DG (2005) Calmodulin-dependent protein kinase kinase-β is an alternative upstream kinase for AMP-activated protein kinase. Cell Metab 2:9–19
5. Woods A, Cheung PC, Smith FC, Davison MD, Scott J, Beri RK, Carling D (1996) Characterization of AMP-activated protein kinase β and γ subunits. Assembly of the heterotrimeric complex in vitro. J Biol Chem 271:10282–10290
6. Polekhina G, Gupta A, Michell BJ, van Denderen B, Murthy S, Feil SC, Jennings IG, Campbell DJ, Witters LA, Parker MW, Kemp BE, Stapleton D (2003) AMPK β subunit targets metabolic stress sensing to glycogen. Curr Biol 13:867–871
7. Adams J, Chen ZP, Van Denderen BJ, Morton CJ, Parker MW, Witters LA, Stapleton D, Kemp BE (2004) Intrasteric control of AMPK via the γ1 subunit AMP allosteric regulatory site. Protein Sci 13:155–165
8. Cheung PC, Salt IP, Davies SP, Hardie DG, Carling D (2000) Characterization of AMP-activated protein kinase γ-subunit isoforms and their role in AMP binding. Biochem J 346:659–669
9. Oakhill JS, Chen ZP, Scott JW, Steel R, Castelli LA, Ling N, Macaulay SL, Kemp BE (2010) β-Subunit myristoylation is the gatekeeper for initiating metabolic stress sensing by AMP-activated protein kinase (AMPK). Proc Natl Acad Sci USA 107:19237–19241
10. Wojtaszewski JF, Nielsen P, Hansen BF, Richter EA, Kiens B (2000) Isoform-specific and exercise intensity-dependent activation of 5′-AMP-activated protein kinase in human skeletal muscle. J Physiol 528:221–226
11. Fujii N, Hayashi T, Hirshman MF, Smith JT, Habinowski SA, Kaijser L, Mu J, Ljungqvist O, Birnbaum MJ, Witters LA, Thorell A, Goodyear LJ (2000) Exercise induces isoform-specific increase in 5′AMP-activated protein kinase activity in human skeletal muscle. Biochem Biophys Res Commun 273:1150–1155
12. Minokoshi Y, Kim YB, Peroni OD, Fryer LG, Müller C, Carling D, Kahn BB (2002) Leptin stimulates fatty-acid oxidation by activating AMP-activated protein kinase. Nature 415:339–343
13. Yamauchi T, Kamon J, Minokoshi Y, Ito Y, Waki H, Uchida S, Yamashita S, Noda M, Kita S, Ueki K, Eto K, Akanuma Y, Froguel P, Foufelle F, Ferre P, Carling D, Kimura S, Nagai R, Kahn BB, Kadowaki T (2002) Adiponectin stimulates glucose utilization and fatty-acid oxidation by activating AMP-activated protein kinase. Nat Med 8:1288–1295
14. Kelly M, Gauthier MS, Saha AK, Ruderman NB (2009) Activation of AMP-activated protein kinase by interleukin-6 in rat skeletal muscle: association with changes in cAMP, energy state, and endogenous fuel mobilization. Diabetes 58:1953–1960
15. Matthews VB, Aström MB, Chan MH, Bruce CR, Krabbe KS, Prelovsek O, Akerström T, Yfanti C, Broholm C, Mortensen OH, Penkowa M, Hojman P, Zankari A, Watt MJ, Bruunsgaard H, Pedersen BK, Febbraio MA (2009) Brain-derived neurotrophic factor is produced by skeletal muscle cells in response to contraction and enhances fat oxidation via activation of AMP-activated protein kinase. Diabetologia 52:1409–1418
16. Suwa M, Egashira T, Nakano H, Sasaki H, Kumagai S (2006) Metformin increases the PGC-1α protein and oxidative enzyme activities possibly via AMPK phosphorylation in skeletal muscle in vivo. J Appl Physiol 101:1685–1692
17. LeBrasseur NK, Kelly M, Tsao TS, Farmer SR, Saha AK, Ruderman NB, Tomas E (2006) Thiazolidinediones can rapidly activate AMP-activated protein kinase in mammalian tissues. Am J Physiol Endocrinol Metab 291:E175–E181
18. Merrill GF, Kurth EJ, Hardie DG, Winder WW (1997) AICA riboside increases AMP-activated protein kinase, fatty acid oxidation, and glucose uptake in rat muscle. Am J Physiol 273:E1107–E1112
19. Jessen N, Pold R, Buhl ES, Jensen LS, Schmitz O, Lund S (2003) Effects of AICAR and exercise on insulin-stimulated glucose uptake, signaling, and GLUT-4 content in rat muscles. J Appl Physiol 94:1373–1379
20. Kitaoka Y, Takahashi Y, Machida M, Takeda K, Takemasa T, Hatta H (2014) Effect of AMPK activation on monocarboxylate transporter (MCT)1 and MCT4 in denervated muscle. J Physiol Sci 64:59–64
21. Suwa M, Nakano H, Kumagai S (2003) Effects of chronic AICAR treatment on fiber composition, enzyme activity, UCP3, and PGC-1 in rat muscles. J Appl Physiol 95:960–968
22. Winder WW, Holmes BF, Rubink DS, Jensen EB, Chen M, Holloszy JO (2000) Activation of AMP-activated protein kinase increases mitochondrial enzymes in skeletal muscle. J Appl Physiol 88:2219–2226
23. Brandauer J, Vienberg SG, Andersen MA, Ringholm S, Risis S, Larsen PS, Kristensen JM, Frøsig C, Leick L, Fentz J, Jørgensen S, Kiens B, Wojtaszewski JF, Richter EA, Zierath JR, Goodyear LJ, Pilegaard H, Treebak JT (2013) AMP-activated protein kinase regulates nicotinamide phosphoribosyl transferase expression in skeletal muscle. J Physiol 591:5207–5220
24. Suwa M, Nakano H, Radak Z, Kumagai S (2011) Short-term adenosine monophosphate-activated protein kinase activator 5-aminoimidazole-4-carboxamide-1-β-D-ribofuranoside treatment increases the sirtuin 1 protein expression in skeletal muscle. Metabolism 60:394–403
25. Motta MC, Divecha N, Lemieux M, Kamel C, Chen D, Gu W, Bultsma Y, McBurney M, Guarente L (2004) Mammalian SIRT1 represses forkhead transcription factors. Cell 116:551–563
26. Vaziri H, Dessain SK, Ng Eaton E, Imai SI, Frye RA, Pandita TK, Guarente L, Weinberg RA (2001) *hSIR2*^{SIRT1} functions as an NAD-dependent p53 deacetylase. Cell 107:149–159
27. Yeung F, Hoberg JE, Ramsey CS, Keller MD, Jones DR, Frye RA, Mayo MW (2004) Modulation of NF-κB-dependent transcription and cell survival by the SIRT1 deacetylase. EMBO J 23:2369–2380
28. Rodgers JT, Lerin C, Haas W, Gygi SP, Spiegelman BM, Puigserver P (2005) Nutrient control of glucose homeostasis through a complex of PGC-1α and SIRT1. Nature 434:113–118
29. Gerhart-Hines Z, Rodgers JT, Bare O, Bare O, Lerin C, Kim SH, Mostoslavsky R, Alt FW, Wu Z, Puigserver P (2007) Metabolic control of muscle mitochondrial function and fatty acid oxidation through SIRT1/PGC-1α. EMBO J 26:1913–1923
30. Fulco M, Cen Y, Zhao P, Hoffman EP, McBurney MW, Sauve AA, Sartorelli V (2008) Glucose restriction inhibits skeletal myoblast differentiation by activating SIRT1 through AMPK-mediated regulation of Nampt. Dev Cell 14:661–673
31. Costford SR, Bajpeyi S, Pasarica M, Albarado DC, Thomas SC, Xie H, Church TS, Jubrias SA, Conley KE, Smith SR (2010) Skeletal muscle NAMPT is induced by exercise in humans. Am J Physiol Endocrinol Metab 298:E117–E126
32. Koltai E, Szabo Z, Atalay M, Boldogh I, Naito H, Goto S, Nyakas C, Radak Z (2010) Exercise alters SIRT1, SIRT6, NAD and

NAMPT levels in skeletal muscle of aged rats. Mech Ageing Dev 131:21–28
33. Suwa M, Sakuma K (2013) The potential role of sirtuins regarding the effects of exercise on aging-related diseases. Curr Aging Sci 6:178–188
34. Pereira Sant'Ana JA, Ennion S, Sargeant AJ, Moorman AF, Goldspink G (1997) Comparison of the molecular, antigenic and ATPase determinants of fast myosin heavy chains in rat and human: a single-fibre study. Pflugers Arch 435:151–163
35. Galler S, Schmitt TL, Pette D (1994) Stretch activation, unloaded shortening velocity, and myosin heavy chain isoforms of rat skeletal muscle fibres. J Physiol 478:513–521
36. Rivero JL, Talmadge RJ, Edgerton VR (1999) Interrelationships of myofibrillar ATPase activity and metabolic properties of myosin heavy chain-based fibre types in rat skeletal muscle. Histochem Cell Biol 111:277–287
37. Delp MD, Duan C (1996) Composition and size of type I, IIA, IID/X, and IIB fibers and citrate synthase activity of rat muscle. J Appl Physiol 80:261–270
38. Takekura H, Yoshioka T (1990) Different metabolic responses to exercise training programmes in single rat muscle fibres. J Muscle Res Cell Motil 11:105–113
39. Chi MM, Hintz CS, Coyle EF, Martin WH 3rd, Ivy JL, Nemeth PM, Holloszy JO, Lowry OH (1983) Effects of detraining on enzymes of energy metabolism in individual human muscle fibers. Am J Physiol 244:C276–C287
40. Takekura H, Yoshioka T (1989) Ultrastructural and metabolic profiles on single muscle fibers of different types after hindlimb suspension in rats. Jpn J Physiol 39:385–396
41. Lee-Young RS, Canny BJ, Myers DE, McConell GK (2009) AMPK activation is fiber type specific in human skeletal muscle: effects of exercise and short-term exercise training. J Appl Physiol 107:283–289
42. Buhl ES, Jessen N, Pold R, Ledet T, Flyvbjerg A, Pedersen SB, Pedersen O, Schmitz O, Lund S (2002) Long-term AICAR administration reduces metabolic disturbances and lowers blood pressure in rats displaying features of the insulin resistance syndrome. Diabetes 51:2199–2206
43. Holmes BF, Kurth-Kraczek EJ, Winder WW (1999) Chronic activation of 5′-AMP-activated protein kinase increases GLUT-4, hexokinase, and glycogen in muscle. J Appl Physiol 87:1990–1995
44. Stoppani J, Hildebrandt AL, Sakamoto K, Cameron-Smith D, Goodyear LJ, Neufer PD (2002) AMP-activated protein kinase activates transcription of the UCP3 and HKII genes in rat skeletal muscle. Am J Physiol Endocrinol Metab 283:E1239–E1248
45. Suwa M, Nakano H, Radak Z, Kumagai S (2008) Endurance exercise increases the SIRT1 and peroxisome proliferator-activated receptor γ coactivator-1α protein expressions in rat skeletal muscle. Metabolism 57:986–998
46. Steinberg GR, Kemp BE (2009) AMPK in health and disease. Physiol Rev 89:1025–1078
47. Suwa M, Nakano H, Higaki Y, Nakamura T, Katsuta S, Kumagai S (2003) Increased wheel-running activity in the genetically skeletal muscle fast-twitch fiber-dominant rats. J Appl Physiol 94:185–192
48. Barnes BR, Marklund S, Steiler TL, Walter M, Hjälm G, Amarger V, Mahlapuu M, Leng Y, Johansson C, Galuska D, Lindgren K, Abrink M, Stapleton D, Zierath JR, Andersson L (2004) The 5′-AMP-activated protein kinase γ3 isoform has a key role in carbohydrate and lipid metabolism in glycolytic skeletal muscle. J Biol Chem 279:38441–38447
49. Mahlapuu M, Johansson C, Lindgren K, Hjälm G, Barnes BR, Krook A, Zierath JR, Andersson L, Marklund S (2004) Expression profiling of the γ-subunit isoforms of AMP-activated protein kinase suggests a major role for γ3 in white skeletal muscle. Am J Physiol Endocrinol Metab 286:E194–E200
50. Nilsson EC, Long YC, Martinsson S, Glund S, Garcia-Roves P, Svensson LT, Andersson L, Zierath JR, Mahlapuu M (2006) Opposite transcriptional regulation in skeletal muscle of AMP-activated protein kinase γ3 R225Q transgenic versus knock-out mice. J Biol Chem 281:7244–7252
51. Garcia-Roves PM, Osler ME, Holmström MH, Zierath JR (2008) Gain-of-function R225Q mutation in AMP-activated protein kinase γ3 subunit increases mitochondrial biogenesis in glycolytic skeletal muscle. J Biol Chem 283:35724–35734
52. Cantó C, Jiang LQ, Deshmukh AS, Mataki C, Coste A, Lagouge M, Zierath JR, Auwerx J (2010) Interdependence of AMPK and SIRT1 for metabolic adaptation to fasting and exercise in skeletal muscle. Cell Metab 11:213–219
53. Treebak JT, Glund S, Deshmukh A, Klein DK, Long YC, Jensen TE, Jørgensen SB, Viollet B, Andersson L, Neumann D, Wallimann T, Richter EA, Chibalin AV, Zierath JR, Wojtaszewski JF (2006) AMPK-mediated AS160 phosphorylation in skeletal muscle is dependent on AMPK catalytic and regulatory subunits. Diabetes 55:2051–2058
54. Cantó C, Gerhart-Hines Z, Feige JN, Lagouge M, Noriega L, Milne JC, Elliott PJ, Puigserver P, Auwerx J (2009) AMPK regulates energy expenditure by modulating NAD^+ metabolism and SIRT1 activity. Nature 458:1056–1060
55. Guerra B, Guadalupe-Grau A, Fuentes T, Ponce-González JG, Morales-Alamo D, Olmedillas H, Guillén-Salgado J, Santana A, Calbet JA (2010) SIRT1, AMP-activated protein kinase phosphorylation and downstream kinases in response to a single bout of sprint exercise: influence of glucose ingestion. Eur J Appl Physiol 109:731–743
56. Ljubicic V, Khogali S, Renaud JM, Jasmin BJ (2012) Chronic AMPK stimulation attenuates adaptive signaling in dystrophic skeletal muscle. Am J Physiol Cell Physiol 302:C110–C121
57. Gurd BJ, Yoshida Y, Lally J, Holloway GP, Bonen A (2009) The deacetylase enzyme SIRT1 is not associated with oxidative capacity in rat heart and skeletal muscle and its overexpression reduces mitochondrial biogenesis. J Physiol 587:1817–1828
58. Putman CT, Kiricsi M, Pearcey J, MacLean IM, Bamford JA, Murdoch GK, Dixon WT, Pette D (2003) AMPK activation increases uncoupling protein-3 expression and mitochondrial enzyme activities in rat muscle without fibre type transitions. J Physiol 551:169–178
59. Wang P, Zhang RY, Song J, Guan YF, Xu TY, Du H, Viollet B, Miao CY (2012) Loss of AMP-activated protein kinase-α2 impairs the insulin-sensitizing effect of calorie restriction in skeletal muscle. Diabetes 61:1051–1061
60. Corton JM, Gillespie JG, Hawley SA, Hardie DG (1995) 5-aminoimidazole-4-carboxamide ribonucleoside. A specific method for activating AMP-activated protein kinase in intact cells? Eur J Biochem 229:558–565
61. Guigas B, Bertrand L, Taleux N, Foretz M, Wiernsperger N, Vertommen D, Andreelli F, Viollet B, Hue L (2006) 5-Aminoimidazole-4-carboxamide-1-β-D-ribofuranoside and metformin inhibit hepatic glucose phosphorylation by an AMP-activated protein kinase-independent effect on glucokinase translocation. Diabetes 55:865–874
62. Longnus SL, Wambolt RB, Parsons HL, Brownsey RW, Allard MF (2003) 5-Aminoimidazole-4-carboxamide 1-β-d-ribofuranoside (AICAR) stimulates myocardial glycogenolysis by allosteric mechanisms. Am J Physiol Regul Integr Comp Physiol 284:R936–R944
63. Park S, Kim DS, Kang S, Shin BK (2014) Chronic activation of central AMPK attenuates glucose-stimulated insulin secretion and exacerbates hepatic insulin resistance in diabetic rats. Brain Res Bull 108:18–26

64. Lihn AS, Jessen N, Pedersen SB, Lund S, Richelsen B (2004) AICAR stimulates adiponectin and inhibits cytokines in adipose tissue. Biochem Biophys Res Commun. 316:853–858
65. Lihn AS, Pedersen SB, Lund S, Richelsen B (2008) The anti-diabetic AMPK activator AICAR reduces IL-6 and IL-8 in human adipose tissue and skeletal muscle cells. Mol Cell Endocrinol 292:36–41
66. Steinberg GR, Michell BJ, van Denderen BJ, Watt MJ, Carey AL, Fam BC, Andrikopoulos S, Proietto J, Görgün CZ, Carling D, Hotamisligil GS, Febbraio MA, Kay TW, Kemp BE (2006) Tumor necrosis factor α-induced skeletal muscle insulin resistance involves suppression of AMP-kinase signaling. Cell Metab 4:465–474
67. Zhang Z, Zhao M, Li Q, Zhao H, Wang J, Li Y (2009) Acetyl-L-carnitine inhibits TNF-α-induced insulin resistance via AMPK pathway in rat skeletal muscle cells. FEBS Lett 583:470–474

JAFIB

Original Research

Journal of Atrial Fibrillation

www.jafib.com

Impaired Erythrocyte Deformability in Patients with Coronary Risk Factors: Significance of Nonvalvular Atrial Fibrillation

Keita Odashiro, MD[1], Toru Maruyama, MD[2], Taku Yokoyama, MD[1], Hisataka Nakamura, MD[1], Mitsuhiro Fukata, MD[1], Shioto Yasuda, MD[1], Kazuyuki Saito, MD[3], Takehiko Fujino, MD[4], and Koichi Akashi, MD[1]

[1]Department of Medicine, and [2]Faculty of Art and Science, Kyushu University, [3]BOOCS Clinic, [4]Institute of Rheological Function of Foods Co. Ltd., Fukuoka, Japan.

Abstract

Although coronary risk factors promote the formation of atherosclerotic plaque containing activated platelets and inflammatory leukocytes, and play a pivotal role in the development of coronary artery diseases (CAD), the hemorheological effects of these risk factors on circulating intact erythrocytes, a major component of whole blood cells, are poorly understood. Therefore, this study aimed to quantify erythrocyte deformability in patients with coronary risk factors, and enrolled 320 consecutive cardiac outpatients including 33 patients with nonvalvular atrial fibrillation (AF). Patients with acute coronary syndrome or valvular AF were excluded. Demographic variables obtained by medical records were correlated with erythrocyte deformability investigated by our highly sensitive and reproducible filtration technique. Among demographic variables, triglyceride ($p = 0.004$), HbA1c ($p = 0.014$) and body weight ($p = 0.020$) showed significant inverse correlation to the erythrocyte deformability. This deformability was not associated with types of CAD (old myocardial infarction vs. stable angina) or modality of treatment (percutaneous intervention vs. coronary artery bypass grafting). Unexpectedly, stepwise multiple regression analysis demonstrated that nonvalvular AF was the most significant contributor to the impaired erythrocyte deformability ($p = 0.002$). Hypertension and dyslipidemia are more prevalent in the AF patients ($p < 0.001$), and the erythrocyte deformability was found to be impaired synergistically and significantly ($p < 0.001$) during the stepwise accumulation of the coronary risk factors in addition to AF. In conclusion coronary risk factors synergistically impair the erythrocyte deformability, which may play an important role in critically stenotic coronary arteries. Since the impairment of intact erythrocyte deformability is mostly associated with nonvalvular AF, this common arrhythmia may reflect the coronary risk accumulation.

Introduction

Hemorheology in association with coronary atherosclerotic plaque formation has drawing increasing attention. Much effort has been devoted to elucidate the role of activated platelets and leukocyte (scavenger macrophages, activated lymphocytes and inflammatory polymorphonuclear neutrophils) in atherosclerotic progression and prothrombotic tendencies. In contrast, the effects of coronary risk factors on the behaviors of circulating intact erythrocytes, major component of whole blood cells, have been poorly understood in actual cardiac patients. The deformability of erythrocytes that pass through the microvascular network is an essential factor to maintain the physiological fluent microcirculation. Physiological and hematological values of erythrocyte deformability are equivalent to those of platelet aggregating and leukocyte migratory functions. However, the concept of erythrocyte deformability has not been strictly defined as a physical quantity, and the evaluation of deformability depends on the measurement technique and its relative sensitivity.[1] Erythrocytes deformability is supposed to be impaired in patients with coronary artery disease (CAD) by mechanical stress depending on plaque morphology such as irregular surface, calcified plaque edge and sharp plaque shoulder. This deformability is also impaired by shear stress of high blood flow velocity observed in stenotic coronary arteries. Nevertheless, erythrocytes deformability is a fundamental prerequisite of coronary microcirculation maintaining patency of critically stenotic coronary arteries or collateral circulation.[2] Therefore, the aim of this study is to investigate the homerheologic effects of coronary risk factors on the intact erythrocyte deformability, using our highly sensitive and reproducible filtration technique. In this setting, erythrocyte

Key Words:
Atrial fibrillation, Coronary risk factors, Deformability, Erythrocytes

Disclosures:
Done.

Corresponding Author:
Toru Maruyama, MD., PhD.
Faculty of Art and Science
Kyushu University
Kasuga Kohen 6-1, Kasuga 816-8580
Japan.

deformability is considered as filterability of erythrocyte suspension. As mMicropipette technique, a representative hemorheologic methods other than filtration technique, estimates single erythrocyte membrane rigidity, one of the components regulating whole cell deformability.[3] Therefore, erythrocyte suspension filterability is considered as whole cell deformabilty.

Methods

Study Population

This study was approved by the internal ethics committee of the Institute of Rheological Function of Foods Co. Ltd. (Fukuoka, Japan) and was performed in accordance with the Declaration of Helsinki, i.e., signed informed consent was obtained from each subject prior to enrollment into the study. The study population consisted of 320 Japanese patients (209 males and 111 females) with common cardiac and/or systemic diseases. All patients were managed monthly at least over 1.5 years and treated at the discretion of attending physicians in the outpatients section of the Kyushu University Hospital (Fukuoka, Japan) or in several teaching hospitals and community clinics affiliated to the University Hospital. Hypertension was defined as casual blood pressure > 140/90 mmHg or treatment with antihypertensive drugs. Type 2 diabetes mellitus was defined as fasting serum glucose > 126 mg/dl, casual serum glucose > 200 mg/dl, HbA1c(NGSP) > 6.5% and/or current antidiabetic medication.4 Patients with type 1 diabetes mellitus were not enrolled. Dyslipidemia was defined as serum LDL cholesterol > 140 mg/dl, serum HDL cholesterol < 40 mg/dl or prescription of lipid-lowering agents.[4] Coronary artery disease (CAD) included old myocardial infarction and stable angina pectoris irrespective of conservative, endovascular or surgical treatment. Activity of CAD was stable in these patients and those with acute coronary syndrome (ACS) were excluded. Chronic kidney disease (CKD) covers all the stages of impaired renal function, indicating estimated glomerular filtration rate (eGFR) ≤ 60 ml/min/1.73m2.[5] Patients with atrial fibrillation (AF) due to evident rheumatic mitral valve diseases, episode of mitral valve replacement or valvuloplasty were excluded. Therefore, AF was nonvalvular. Paroxysmal AF was defined according to the HRS/EHRA/ECAS 2012 Consensus Statement on Catheter and Surgical Ablation of AF.[6] In this Consensus Statement, the concept of permanent AF was considered inappropriate in that patient and physician ceased further attempts to restore and maintain sinus rhythm, whenever this joint decision is made. However, the term of permanent AF, defined as longstanding AF impossible to be terminated by any means, was used in this study in contrast to paroxysmal AF. AF outpatients (n = 33) were followed every month for anticoagulation, i.e., 20 patients showed permanent AF whereas 13 patients had paroxysmal AF. In AF patients treated with warfarin, time in therapeutic range (TTR) of the international normalized ratio of prothrombin time (PT-INR) ranged from 51 to 72% (65.6 ± 0.9%). Dabigatran (n = 7) and rivaroxaban (n = 5) were also prescribed newly or converted from warfarin. Transthoracic echocardiography and Holter monitoring were conducted in all AF patients. Treatment of the aforementioned coronary risk factors was under the discretion of the treating physicians in outpatient clinics. Medication and lifestyle including smoking were not altered in any patient during the study period.

Erythrocyte Filterability

Erythrocyte suspensions were prepared as described elsewhere.[7] In brief, venous blood (approximately 10 ml) was sampled in the morning after an overnight fast. Blood cell counting and hematocrit measurement were performed using a hemocytometer (Ace Counter, FLC-240A, Fukuda Denshi Co. Ltd., Tokyo, Japan). After centrifugation at 1300 x g for 10 min, supernatant was aspirated to replace buffy coat and plasma with HEPES-buffered saline. Intact erythrocytes were then washed three times (800 x g, 600 x g and 500 x g for 10 min each) by re-suspension with HEPES-buffered saline and the final hematocrit of erythrocyte suspension was adjusted to 3.0% to prevent erythrocytes sticking within the filter pores and to reuse the specific filter. These procedures were performed within 2 hours after blood sampling for subsequent filtration experiments.[7]

Erythrocyte filterability (whole cell deformability) was investigated blindly by filtration technique (Model NOBU-II, Tsukasa Sokken Co. Ltd., Tokyo, Japan) as reported elsewhere.[8,9] Nickel mesh filters were produced by a photo-fabrication technique (Dainippon Printing Co. Ltd., Tokyo, Japan) and characterized by regularly distributed pores of identical size and shape (Fig. 1A), which guarantees the sensitivity of filtration experiments even in the erythrocyte suspension with low (3.0%) hematocrit value. A specific filter with appropriate pore size (4.94 μm in diameter) was used repetitively by sonication during a series of experiments to guarantee the reproducibility. The relationship between hydrostatic pressure (P; mmH2O) and time (t; sec) was obtained during continuous filtration under gravity using a pressure transducer. P was transformed to the height of the meniscus in the vertical tube (h; mm) and flow rate (Q; ml/min) was calculated by the rate of fall of the meniscus ($\Delta h/\Delta t$) and internal cross-sectional area of the vertical tube. P-Q relationship was obtained automatically by software installed on a personal computer (DELL Latitude CS, Dell Inc., Round Rock, TX, USA) and stored simultaneously on Microsoft Office Excel 2003 on Windows XP (Microsoft, Tokyo, Japan). The percentage of Q of erythrocyte suspension relative to Q of saline at 100 mmH2O was used as an index of erythrocyte filterability. Temperature of the specimens was kept at 25°C by circulating isothermal water within a water jacket around the

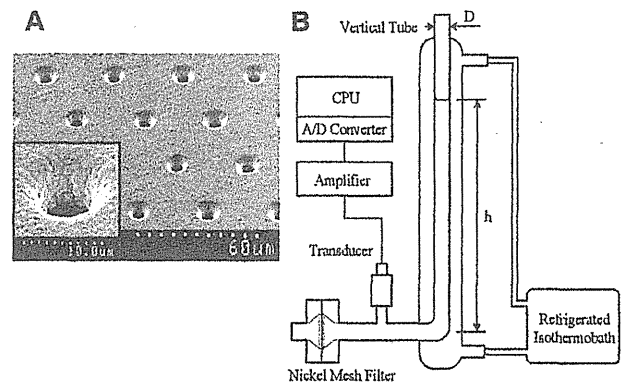

Figure 1: **A: Scanning electron microscopic photograph of a nickel mesh filter. Inset shows magnification of a single pore in this filter. B: Schematic illustration of nickel mesh filtration system. Filtration pressure (P; mmH2O) is converted to the height of the meniscus within the vertical tube (h; mm) using the equation h = P/ρg. Flow rate (Q; ml/min) is calculated using the equation Q = π(D/2)2(Δh/Δt). D, internal diameter of vertical tube; Δh/Δt, first time derivatives of h; g, acceleration of gravity; ρ, specific gravity of specimens.**

vertical tube (Fig. 1B). These examinations were performed at room temperature (22 ± 2°C).

An aliquot of the erythrocyte suspension was fixed with isotonic 1.0% glutaraldehyde solution containing 24.5 mM NaCl and 50 mM phosphate buffer (pH 7.4). Thereafter, the shape of erythrocytes was observed blindly using a differential interference contrast microscope (Diaphoto 300, Nikon Co. Ltd., Tokyo, Japan) at 400 x magnification.

Data Analyses

All data are expressed as means ± SEM. For statistical analyses, human sample size was chosen to provide 90% power with an α error of 0.05. A total of ≥ 310 cases was required provided that the significant intergroup difference of human erythrocyte filterability investigated by this technique is 1.0%.[9] Continuous variables were compared with unpaired Student's t test or Mann-Whitney U test. Erythrocyte filterability (%) was compared by the latter, because Kolmogorov-Smirnov test confirmed that this was not normally distributed ($p < 0.001$). Discrete variables were analyzed by Fisher's exact test or Pearson's $\chi 2$ test. Linear regression was fitted by the standard least square method. Significant contributors to erythrocyte filterability impairment were determined by stepwise multiple regression analysis. None of the variables with missing data qualified. The criteria for entering into the regression model were significant partial correlation coefficient (r) to the filterability, greatest r among the same category even if it was not significant, or otherwise clinically meaningful variables. These analyses were performed using Predictive Analytics Software (PASW) 18.0 version for Windows (SPSS, Inc., IBM, Chicago, IL, USA). Differences with two-sided $p < 0.05$ were considered significant.

Results

Patients' Profile

Baseline characteristics of enrolled subjects are detailed in Table 1. Averages of some listed variables had already reached the upper limit of normal range (systolic blood pressure) or even exceeded the ranges (HbA1c, fasting serum glucose, triglyceride). None of these patients had experienced an episode of evident heart failure (NYHA class ≥III). In patients with CAD, 25 patients had a history of old myocardial infarction and the remaining 23 patients showed stable angina pectoris. Percutaneous coronary intervention (PCI) was performed in 38 patients, and coronary artery bypass grafting surgery (CABG) was conducted in 21 patients. Medication included Ca antagonists (n = 46, 14%), statins (n = 34, 11%), angiotensin receptor blockers (n = 28, 9%), antiplatelet agents (n = 27, 8%), β-blockers (n = 18, 6%), angiotensin converting enzyme inhibitors (n = 16, 5%) and do on.

Table 1: Baseline Characteristics of Subjects (N = 320)

Variables	Means ± SEM	Variables	Means ± SEM
Age (years)	61.5 ± 0.7	LDL cholesterol (mg/dl)	120 ± 2
Body weight (kg)	62.6 ± 0.7	Triglyceride (mg/dl)	160 ± 8
Fat (%)	27.2 ± 0.5	WBC (x 102/μl)	60.2 ± 1.1
BMI (kg/m2)	24.2 ± 0.2	RBC (x 104/μl)	442 ± 3
SBP (mmHg)	140 ± 1	Hb (g/dl)	14.1 ± 0.1
DBP (mmHg)	80 ± 1	Ht (%)	40.9 ± 0.3
HbA1c (%)	7.0 ± 0.1	MCH (pg)	31.9 ± 0.1
FSG (mg/dl)	149 ± 3	MCV (fl)	92.7 ± 0.3
Total Cholesterol (mg/dl)	208 ± 2	MCHC (g/dl)	34.4 ± 0.1
HDL cholesterol (mg/dl)	56 ± 1	Erythrocyte filterability (%)	87.6 ± 0.2

BMI, body mass index; DBP, diastolic blood pressure; FSG, fasting serum glucose; MCH, mean corpuscular hemoglobin; MCHC, mean corpuscular hemoglobin concentration; MCV, mean corpuscular volume; SBP, systolic blood pressure.

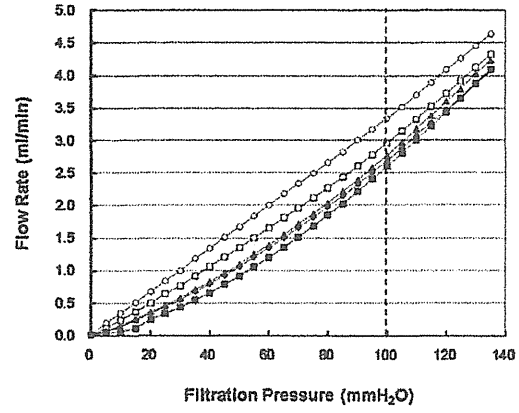

Figure 2A: A: Representative P-Q relationships during continuous filtration experiment using erythrocyte suspensions and HEPES-buffered saline. The P-Q relationships with open symbols correspond to filtrations of saline (open circles) or erythrocyte suspension obtained from a healthy non-smoker without coronary risk factors (open squares). Closed symbols indicate representative patients with diabetes (closed triangles), dyslipidemia (closed diamonds) and permanent atrial fibrillation (closed squares). Q in patients with these diseases (closed symbols) is less than Q in a subject without them (open squares) at any given P. B: Magnification of the P-Q curves at filtration pressure around 100 mmH2O.

Representative Filtration Data

Hematologically, there were no remarkable erythrocytes shape changes observed in the enrolled subjects. Figure 2 shows representative results of the nickel mesh filtration experiments. The continuous filtration process yielded P-Q relationships for control

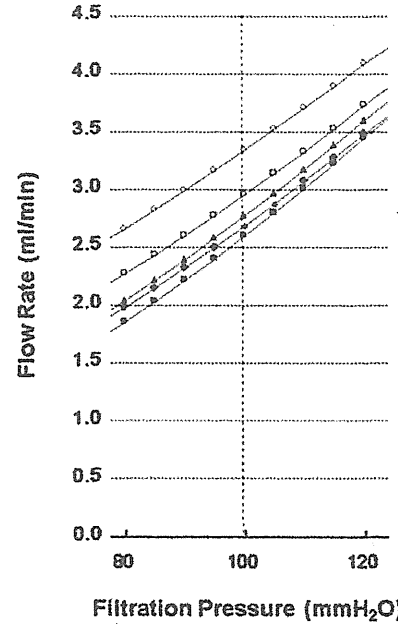

Figure 2B: B: Magnification of the P-Q curves at filtration pressure around 100 mmH2O.

Table 2: Correlation of Categorical Factors and Erythrocyte Filterability

Factors		n	Erythrocyte filterability (%)	p
Gender	male	209	87.4 ± 0.2	
	female	111	88.0 ± 0.3	0.072
Current Smoking	(–)	201	87.9 ± 0.2	
	(+)	119	87.2 ± 0.3	0.059
Hypertension	(–)	213	87.6 ± 0.2	
	(+)	107	87.8 ± 0.3	0.867
Dyslipidemia	(–)	217	87.6 ± 0.2	
	(+)	103	87.7 ± 0.3	0.841
Atrial fibrillation	(–)	287	87.8 ± 0.2	
	(+)	33	86.3 ± 0.9	0.308
Diabetes mellitus	(–)	100	88.1 ± 0.2	
	(+)	220	87.4 ± 0.2	0.200
CKD	(–)	184	87.9 ± 0.2	
	(+)	136	87.2 ± 0.3	0.041
CAD	(–)	272	88.2 ± 0.2	
	(+)	48	87.5 ± 0.3	0.407

Erythrocyte filterability is expressed as mean ± SEM. CAD, coronary artery disease; CKD, chronic kidney disease;
n, number of subjects in a specific group; p, probability.

saline and erythrocyte suspensions. Reproducibility of the filtration experiment was confirmed in that P-Q curves obtained by filtration of the same specimen were superimposable as in our recent study.[8,9] Saline demonstrated a linear P-Q relationship passing through the origin, which is compatible with Newtonian fluid. P-Q relationships for the erythrocyte suspensions displayed smooth and upward concave curves over the low-pressure region. These findings indicate that erythrocyte suspension shows non-Newtonian behavior, which is evident under a low-shear-rate condition. Open squares correspond to erythrocyte suspensions obtained from subjects without any coronary risk factors. Closed symbols indicate those obtained from patients with at least one risk factor. Q of erythrocyte suspensions obtained from patients with these risk factors were always less than Q in patients without them at any given pressure. These findings indicate that these coronary risk factors impair the human erythrocyte filterability.

Table 3: Correlation of Continuous Variables and Erythrocyte Filterability

	(N = 320)	
Variables	r	p
Age (years)	0.041	0.460
Body weight (kg)	–0.130	0.020
BMI (kg/m2)	–0.094	0.095
Fat (%)	–0.074	0.293
SBP (mmHg)	–0.033	0.557
DBP (mmHg)	–0.027	0.639
HbA1c (%)	–0.137	0.014
Total cholesterol (mg/dl)	–0.062	0.271
HDL cholesterol (mg/dl)	0.100	0.076
LDL cholesterol (mg/dl)	–0.101	0.073
Triglyceride (mg/dl)	–0.159	0.004
MCH (pg)	–0.014	0.798
MCV (fl)	–0.018	0.742
MCHC (g/dl)	0.003	0.954

.p, probability; r, partial correlation coefficient. Other abbreviations are the same as in Table 1.

Erythrocyte Filterability and Coronary Risk Factors

Relationships between categorical factors and erythrocyte filterability are shown in Table 2. CKD alone showed significant impairment of erythrocyte filterability ($p = 0.041$). The filterability in AF patients did not differ from that in the remaining subjects, and the filterability in permanent AF was equivalent to that in paroxysmal AF. Correlations of continuous variables and erythrocyte filterability are demonstrated in Table 3. Body weight, HbA1c and triglyceride showed significant inverse correlation, whereas hematological parameters relating to erythrocyte size (mean corpuscular volume; MCV) and internal density (mean corpuscular hemoglobin concentration; MCHC) did not show any correlation with filterability.

Prior to the multiple regression analysis, demographic variables suitable for inclusion into the regression model were selected. For categorical variables, CKD was selected for significance ($p = 0.041$), current smoking was included as a potent risk of hemorheology,10 and AF was selected as an outcome of overall risk accumulation.6 For continuous variables, body mass index (BMI, $p = 0.095$) instead of body weight ($p = 0.020$) was selected as a surrogate of obesity. HbA1c ($p = 0.014$) and triglyceride ($p = 0.004$) were selected for respective significance. Although hematological indices were not significant, MCV was selected for its greatest r.

Multiple regression analysis was performed to identify significant covariates contributing to the impairment of erythrocyte filterability with concurrent avoidance of multi-colinearity by monitoring the variance inflation factors. Table 4 shows five regression models including selected continuous or categorical variables according to stepwise reduction. Multiple correlation coefficients were highly significant in this series of regression models. AF was the greatest contributor to the impaired erythrocyte filterability in all the listed models with high significance ($p = 0.002 - 0.023$).

Erythrocyte filterability of AF patients did not differ from that of the remaining patients (Table 2). However, AF remained alone as the greatest contributor to the impaired erythrocyte filterability (Table 4). Table 5 shows the distribution of AF in patients with coronary risk factors. AF was prevalent significantly ($p < 0.001$) in hypertensive and dyslipidemic patients. Table 6 further indicates the effects of coronary risk accumulation on the erythrocyte filterability. Multiple comparison of the filterability under the stepwise accumulation of coronary risk factors showed highly significance ($p < 0.001$), i.e., the erythrocyte filterability was impaired synergistically during the accumulation of coronary risk factors in addition to AF. However, the filterability was not different with respect to the types of CAD (old myocardial infarction vs. stable angina), modality of treatment (PCI vs. CABG), and choice of medication (not shown).

Discussion

Main Findings

The erythrocyte deformability has significant impact on the apparent blood viscosity, which has profound influence on the coronary blood flow,2 development of myocardial infarction and the resultant infarct size.[11] However, the involvement of abnormal erythrocyte behaviors

Table 4: Stepwise Multiple Regression Analysis Predicting Contributors to Erythrocyte Filterability (N = 320)

model	F	R	P	Covariates (p)
1	2.650	0.259	0.008	Atrial fibrillation (0.023), Triglyceride (0.025), HbA1c (0.040), BMI (0.295) Current smoking (0.346), MCV (0.367), SBP (0.538), CKD (0.848)
2	3.034	0.259	0.004	Atrial fibrillation (0.023), Triglyceride (0.024), HbA1c (0.036), BMI (0.298) Current smoking (0.346), MCV (0.366), SBP (0.557)
3	4.077	0.273	0.001	Atrial fibrillation (0.004), Triglyceride (0.022), HbA1c (0.061), BMI (0.258) Current smoking (0.224), MCV (0.389)
4	4.748	0.269	< 0.001	Atrial fibrillation (0.003), Triglyceride (0.019), HbA1c (0.088), BMI (0.326) Current smoking (0.177)
5	5.835	0.265	< 0.001	Atrial fibrillation (0.002), Triglyceride (0.010), HbA1c (0.070), Current smoking (0.196)

F, F-value for fitness of multiple linear regression; P, probability for trend toward fitting the regression; p, probability of significant covariate contribution; R, multiple correlation coefficient. Other abbreviations are the same as in Table 1.

on the progression of CAD is not fully elucidated. In the present study, a highly sensitive and reproducible filtration technique was applied to the actual cardiac outpatients to assess the circulating intact erythrocyte filterability (whole cell deformability) in relation to coronary risk factors. Univariate analyses found significant impact of triglyceride (p = 0.004), HbA1c (p = 0.014), body weight (p = 0.020), and CKD (p = 0.041) on the impairment of the erythrocyte deformability, but multiple regression analysis demonstrated that nonvalvular AF was the greatest contributor to the impaired deformability, indicating that coronary risk factors including AF impair the erythrocyte filterability synergistically.

Erythrocyte Deformability and Coronary Risk Factors

It is generally accepted that erythrocyte deformability is determined by 1) erythrocyte membrane material properties; 2) internal density as reflected by MCHC; and 3) cellular geometric factors as reflected by MCV, surface-to-volume ratio and erythrocyte shape.[1] Therefore, abnormal erythrocyte membrane properties, increased MCHC or MCV, and several kinds of shape changes impair the deformability individually or in concert. There were no discernible erythrocyte shape changes in this study population. There were contributions of AF, triglyceride and HbA1c, but not of MCV or MCHC, to the deformability (Tables 3, 4). These findings indicate that impaired deformability mainly arises from erythrocyte membrane properties which may be altered by coronary risk factors such as hypertension, dyslipidemia, diabetes in addition to smoking.[10]

Erythrocyte membrane lipid components have profound influence on membrane fluidity and hemorheologic functions.[1] The present study demonstrated the association of impaired deformability with elevated serum triglyceride as in our previous study,[7] suggesting altered erythrocyte membrane integrity and lipid composition in hypertriglyceridemia.[12] Reportedly, our recent study clarified that diabetic erythrocytes show the impaired filterability and this impairment is enhanced by other risk factor such as smoking causing potent oxidative stress.[9,10] In this study, HbA1c is inversely proportional to the filterability (Table 3) and a marginal contributor to the impaired filterability (Table 4). Tsuda[13] demonstrated the increased erythrocyte membrane rigidity in hypertensive patients by electron spin resonance study. Therefore, the main cause of the impaired erythrocyte filterability is attributed to the erythrocyte membrane abnormalities in diabetic, hypertensive or dyslipidemic patients. Previous studies using this filtration technique (Fig. 1) clarified that deformability is markedly impaired in human erythrocytes exposed to acute oxidant stress.[14-16] Relative to such severe oxidant stress in vitro, mild oxidant stress in vivo as in above common diseases also causes persistent erythrocyte membrane lipid peroxidation and disturbs deformability.[9,17]

Erythrocyte Deformability in AF

Development of nonvalvular AF is known to be accelerated by risk factors common to those of CAD, because $CHADS_2$ and CHA_2DS_2-VASc scores predict not only the risk of ischemic stroke but also the new onset of AF.[18] Actually, more than half of enrolled patients are diabetic (69%), and one third of them are current smokers (37%) in the present study (Table 2). Moreover, major coexisting diseases are CKD (43%), hypertension (33%), dyslipidemia (32%) and CAD (15%). In this meaning, patients' profile of this study is similar to the Fushimi AF Registry, which is a Japanese domestic survey of AF patients conducted in urban community.[19]

AF is a common arrhythmia in clinical practice, and characterized by abnormal hemorheology in left atrium (LA) such as elevated hematocrit value and fibrinogen concentration.[20,21] Stagnant blood within the enlarged fibrillating LA appendage shows procoagulative state under erythrocyte hyperaggregability and elevated platelet reactivity.[22,23] Activated platelets release prostaglandin E2, which enhances calcium entry into erythrocytes leading to the impairment of erythrocyte deformability.[24,25] AF is associated with oxidant stress via increased LA wall superoxide production or angiotensin II type 1 receptor-mediated pathway.[26,27] Such local LA environment oxidizes erythrocytes and impairs the deformability.[15,16] Erythrocyte dynamics are improved by medication such as statin,[28] aspirin,[29] Ca antagonists[15,25] and eicosapentaenoic acid.[30] These agents were prescribed to AF patients associated with CAD for coronary risk reduction and rate control of AF. Such therapeutic effects may have attenuated the impairment of the erythrocyte deformability in AF patients in this study.

It is questionable whether AF is an independent risk of ACS.[31] Reportedly, total cholesterol content of erythrocyte membrane is increased in the patients with ACS,[32] which is ameliorated by statin therapy.[33,34] Increased cholesterol content reduces the erythrocyte membrane fluidity and impairs the deformability leading to erythrocytes aggregation and coronary flow slowing.[35,36] This study excluded patients with ACS, and the answer for this question awaits future cohort investigating erythrocyte deformability in ACS patients with AF and that in ACS patients without AF.

Limitations

This study has several limitations. First limitation is small sample of patients (n = 320) treated at the discretion of attending physicians. Nonvalvular AF with few episodes of paroxysms may

Table 5: Cross Table of Atrial Fibrillation and Coronary Risk Factors

	Hypertension (+)	Dyslipidemia (+)	Diabetes mellitus (+)	Current Smoking (+)
Atrial fibrillation (+) n = 33	24	20	18	16
Atrial fibrillation (–) n = 287	83	83	202	103
N = 320	n = 107	n = 103	n = 220	n = 119
p	< 0.001	< 0.001	0.063	0.156

n, number of subjects in a specific group; N, total number of subjects

Table 6: Effects of Coronary Risk Accumulation on Erythrocyte Filterability

Coronary Risk Factors	Erythrocyte Filterability (%)
no risk factor	88.8 ± 0.3
Hypertension	87.8 ± 0.3
Hypertension + Dyslipidemia	87.4 ± 0.4
Hypertension + Dyslipidemia + Diabetes mellitus	86.9 ± 0.7
Hypertension + Dyslipidemia + Diabetes mellitus + Smoking	86.3 ± 0.9
Hypertension + Dyslipidemia + Diabetes mellitus + Smoking + Atrial fibrillation	86.1 ± 1.0

Multiple comparison of the erythrocyte filterability during the stepwise accumulation of coronary risk factors showed highly significance ($p < 0.001$).

have been dismissed in this study population. Second limitation is a cross-sectional nature of study design. Coronary risk factors were considerably accumulated in the AF patients group in that average CHA_2DS_2-VASc score was 3.30 ± 0.24. However, unlike in the other study,[37] impaired erythrocyte deformability in AF patients could not be correlated to the ischemic stroke in this study partly due to intensive anticoagulation. Finally, erythrocyte filterability shows small intergroup differences and intragroup deviations (Tables 2 and 6). This is due in part to the aforementioned medication, but in other part due to high sensitivity and reproducibility of our methodology. Filtertability of erythrocytes obtained from healthy volunteers (positive control) was 88.8 ± 0.3% (Table 6), and that of erythrocytes exposed to severe oxidant stress was declined to 20% (negative control) leading to filter occlusion or hemolysis.[15] Therefore, our data presented in this study reflects mildly pathological human erythrocyte behaviors leading to impaired but not occluded microcirculation in vivo under treatments.

Conclusions:

This study investigated the intact human erythrocyte deformability in relation to coronary risk factors of actual cardiac patients. Multiple regression analysis showed that nonvalvular AF is unexpectedly and mostly attributable to the impaired erythrocyte deformability among other coronary risk factors, reflecting nonvalvular AF as an outcome of multiple coronary risk accumulations. Therefore, this small sample study should be validated by a future cohort to validate the important hemorheorologic role of erythrocytes playing in prothrombotic state leading to ischemic stroke associated with AF.

Acknowledgments

This work was financially supported in part by research grants from Eisai Pharmaceutical Company (Tokyo, Japan). The authors would like to thank the staff of the Institute of Rheological Function of Foods Co. Ltd. (Hisayama, Fukuoka) for technical assistance and the staff of Kyushu University Hospital, Fukuoka Higashi Hospital, Seishukai Hospital, Miyata Hospital, Munakata Ishikai Hospital, Sawara Hospital and Takano Hospital for clinical assistance. We lost our colleague, Dr. Nobuhiro Uyesaka (Department of Physiology, Nippon Medical University, Tokyo, Japan) during the preparation of this manuscript, and dedicate this work to his memory.

References:

1. Mohandas N, Chasis JA. Red cell deformability, membrane material properties and shape: regulation by transmembrane, skeletal and cytosolic proteins and lipids. Semin Hematol 1993; 30: 171-192.
2. Yaylali YT, Susam I, Demir E, Bor-Kucukatay M, Uludag B, Kilic-Toprak E, Erken G, Dursunoglu D. Increased red blood cell deformability and decreased aggregation as potential adaptive mechanisms in the slow coronary flow phenomenon. Coron Artery Dis 2013; 24: 11-15.
3. Chabanel A, Schachter D, Chien S. Increased rigidity of red blood cell membrane in young spontaneously hypertensive rats. Hypertension 1987; 10: 603-607.
4. Ohta Y, Tsuchihashi T, Onaka U, Hasegawa E. Clustering of cardiovascular risk factors and blood pressure control status in hypertensive patients. Intern Med 2010; 49: 1483-1487.
5. Matsuo S, Imai E, Horio M, Yasuda Y, Tomita K, Nitta K, Yamagata K, Tomino Y, Yokoyama H, Hishida A. Collaborators developing the Japanese equation for estimated GFR: Revised equations for estimated GFR from serum creatinine in Japan. Am J Kidney Dis 2009; 53: 982-992.
6. Calkins H, Kuck KH, Cappato R, Brugada J, Camm AJ, Chen SA, Crijns HJ, Damino RJ, Davies DW, DiMarco J, Edgerton J, Ellenbogen K, Ezekowitz MD, Haines DE, Haïssaguerre M, Hindricks G, Iesaka Y, Jackman W, Jalife J, Jais P, Kalman J, Keane D, Kim YH, Kirchhof P, Klein G, Kottkamp H, Kumagai K, Lindsay BD, Mansour M, Marchlinki FE, McCarthy PM, Mont JL, Morady F, Nademanee K, Nakagawa H, Natale A, Nattel S, Packer DL, Pappone C, Prystowsky E, Raviele A, Reddy V, Ruskin JN, Shemin RJ, Tsao HM, Wilber D. 2012 HRS/EHRA/ECAS expert consensus statement on catheter and surgical ablation of atrial fibrillation: recommendations for patient selection, procedural techniques, patient management and follow-up, definitions, endpoints, and research trial design. Europace2012; 14: 528-606.
7. Ejima J, Ijichi T, Ohnishi Y, Maruyama T, Kaji Y, Kanaya S, Fujino T, Uyesaka N, Ohmura T. Relationship of high-density lipoprotein cholesterol and red blood cell filterability: cross-sectional study of healthy subjects. Clin Hemorheol Microcirc 2000; 22: 1-7.
8. Ariyoshi K, Maruyama T, Odashiro K, Akashi K, Fujino T, Uyesaka N. Impaired erythrocyte filterability of spontaneously hypertensive rats: investigation by nickel mesh filtration technique. Circ J 2010; 74: 129-136.
9. Saito K, Kokawa Y, Fukata M, Odashiro K, Maruyama T, Akashi K, Fujino T. Impaired deformability of erythrocytes in diabetic rat and human: investigation by the nickel-mesh-filtration technique. J Biorheol 2011; 25: 18-26.
10. Padmavathi P, Reddy VD, Kavitha G, Paramahamsa M, Varadacharyulu N. Chronic cigarette smoking alters erythrocyte membrane lipid composition and properties in male human volunteers. Nitric Oxide 2010; 23: 181-186.
11. Cecchi E, Liotta AA, Gori AM, Valente S, Giglioli C, Lazzeri C, Sofi F, Gensini GF, Abbate R, Mannini L. Relationship between blood viscosity and infarct size in patients with ST-segment elevation myocardial infarction undergoing primary percutaneous coronary intervention. Int J Cardiol 2009; 134: 189-194.
12. Mabile L, Piolot A, Boulet L, Fortin LJ, Doyle N, Rodriguez C, Davignon J, Blache D, Lussier-Cacan S. Moderate intake of n-3 fatty acids is associated with stable erythrocyte resistance to oxidative stress in hypertriglyceridemic subjects. Am J Clin Nutr 2001; 74: 449-456.
13. Tsuda K. Oxidative stress and membrane fluidity of red blood cells in hypertensive and normotensive men: an electron spin resonance investigation. Int Heart J 2010; 51: 121-124.
14. Iwata H, Ukeda H, Maruyama T, Fujino T, Sawamura M. Effect of carbonyl compounds on red blood cells deformability. Biochem Biophys Res Comm 2004; 321: 700-706.
15. Okamoto K, Maruyama T, Kaji Y, Harada M, Mawatari S, Fujino T, Uyesaka N. Verapamil prevents impairment in filterability of human erythrocytes exposed to oxidative stress. Jpn J Physiol 2004; 54: 39-46.
16. Uyesaka N, Hasegawa S, Ishioka N, Ishioka R, Shio H, Schechter AN. Effects of superoxide anions on red cell deformability and membrane proteins. Biorheology 1992; 29: 217-229.
17. Ahmed FN, Naqvi FN, Shafiq F. Lipid peroxidation and serum antioxidant enzymes in patients with type 2 diabetes mellitus. Ann NY Acad Sci 2006; 1084:

481-489.
18. Zuo ML, Liu S, Chan KH, Lau KK, Chong BH, Lam KF, Chan YH, Lau YF, Lip GY, Lau CP, Tse HF, Siu CW. The CHADS2 and CHA2DS2-VASc scores predict new occurrence of atrial fibrillation and ischemic stroke. J Interv Card Electrophysiol 2013; 37: 47-54.
19. Akao M, Chun YH, Wada H, Esato M, Hashimoto T, Abe M, Hasegawa K, Tsuji H, Furuke K, on behalf of the Fushimi AF Registry investigators. Current status of clinical background of patients with atrial fibrillation in a community-based survey: The Fushimi AF Registry. J Cardiol 2013; 61: 260-266.
20. Black IW, Chesteman CN, Hopkins AP, Lee LC, Chong BH, Walsh WF. Hematologic correlates of left atrial spontaneous echo contrast and thromboembolism in nonvalvular atrial fibrillation. J Am Coll Cardiol 1993; 21: 451-457.
21. Hwang JJ, Ko FN, Li YH, Ma HM, Wu GJ, Chang H, Wang SM, Schie JT, Tseng YZ, Kuan P. Clinical implications and factors related to left atrial spontaneous echo contrast in chronic nonvalvular atrial fibrillation. Cardiology 1994; 85: 69-75.
22. Muravyov AV, Tikhomirova IA, Maimistova AA, Bulaeva SV. Extra- and intracellular signaling pathways under red blood cell aggregation and deformability changes. Clin Hemorheol Microcirc 2009; 43: 223-232.
23. Willoughby SR, Robert-Thomson RJ, Lim HS, Schultz C, Prabhu A, De Sciscio P, Wong CX, Worthley MI, Sanders P. Atrial platelet reactivity in patients with atrial fibrillation. Heart Rhythm 2010; 7: 1178-1183.
24. Kaestner L, Tabellion W, Lipp P, Bernhardt I. Prostaglandin E2 activates channel-mediated calcium entry in human erythrocytes: an indication for a blood clot formation supporting process. Thromb Haemost 2004; 92: 1269-1272.
25. Oonishi T, Sakashita K, Uyesaka N. Regulation of red blood cell filterability by Ca2+ influx and cAMP-mediated signaling pathways. Am J Physiol 1997; 273: C1828-C1834.
26. Dubley SC Jr, Hoch NE, McCann LA, Honeycutt C, Diamandopoulos L, Fukai T, Harrison DG, Dikalov SI, Langberg J. Atrial fibrillation increases production of superoxide by the left atrium and left appendage: role of the NADPH and xanthine oxidase. Circulation 2005; 112: 1266-1273.
27. Goette A, Bukowska A, Dobrev D, Pfeiffenberger J, Morawietz H, Strugala D, Wiswedel I, Röhl FW, Wolke C, Bergmann S, Bramlage P, Ravens U, Lendeckel U. Acute atrial tachyarrhythmia induces angiotensin II type 1 receptor-mediated oxidative stress and microvascular flow abnormalities in the ventricles. Eur Heart J 2009; 30: 1411-1420.
28. Coccia R, Spadaccio C, Foppoli C, Perluigi M, Covino E, Lusini M, Chello M. The effect of simvastatin on erythrocyte membrane fluidity during oxidative stress induced by cardiopulmonary bypass: a randomized controlled study. Clin Ther 2007; 29: 1706-1717.
29. Bozzo J, Escolar G, Hernandez MR, Galan AM, Ordinas A. Prohemorrhagic potential of dipyrone, ibuprofen, ketorolac and aspirin: mechanisms associated with blood flow and erythrocyte deformability. J Cardiovasc Pharmacol 2001; 38: 183-190.
30. Seki R, Okamura T, Ide T, Kage M, Sata M, Uyesaka N, Maruyama T. Impaired filterability of erythrocytes from patients with chronic hepatitis C and effects of eicosapentaenoic acid on the filterability. J Physiol Sci 2007; 57: 43-49.
31. Desai NR, Giugliano RP. Can we predict outcomes in atrial fibrillation? Clin Cardiol 2012; 35 (Suppl 1): 10-14.
32. Zhang J, Pan L, Xu Y, Wu C, Wang C, Cheng Z, Zhao R. Total cholesterol content of erythrocyte membranes in acute coronary syndrome: correlation with apolipoprotein A-1 and lipoprotein (a). Coron Artery Dis 2011; 22: 145-152.
33. Tziakas DN, Chalikias GK, Stakos D, Tentes IK, Thomaidi A, Chatzikyriakou S, Mitrousi K, Kortsaris AX, Kaski JC, Boudoulas H, Konstantinides S. Statin use is associated with a significant reduction in cholesterol content of erythrocyte membranes. A novel pleiotropic effect? Cardiovasc Drugs Ther 2009; 23: 471-480.
34. Zhong Y, Tang H, Zeng Q, Wang X, Yi G, Meng K, Mao Y, Mao X. Total cholesterol content of erythrocyte membranes is associated with the severity of coronary artery disease and the therapeutic effect of rosuvastatin. Ups J Med Sci 2012; 117: 390-398.
35. Arbel Y, Banai S, Benhorin J, Finkelstein A, Herz I, Halkin A, Keren G, Yedgar S, Barashtein G, Berliner S. Erythrocyte aggregation as a cause of slow flow in patients of acute coronary syndromes. Int J Cardiol 2012; 154: 322-327.
36. Pytel E, Olszewska-Banaszczyk M, Koter-Michalak M, Broncel M. Increased oxidative stress and decreased membrane fluidity in erythrocytes of CAD patients. Biochem Cell Biol 2013; 91: 315-318.
37. Cecchi E, Marcucci R, Poli D, Antonucci E, Abbate R, Gensini GF, Prisco D, Mannini L. Hyperviscosity as a possible risk factor for cerebral ischemic complications in atrial fibrillation patients. Am J Cardiol 2006; 97: 1745-1748.

OPEN

Mortality Benefit of Participation in BOOCS Program

A Follow-Up Study for 15 Years in a Japanese Working Population

Tsutomu Hoshuyama, MD, Keita Odashiro, MD, Mitsuhiro Fukata, MD, Toru Maruyama, MD, Kazuyuki Saito, MD, Chikako Wakana, MS, Michiko Fukumitsu, MS, and Takehiko Fujino, MD

Objective: This study aims to demonstrate the protective effect on mortality among participants of a health education program, Brain-Oriented Obesity Control System (BOOCS). **Methods:** A quasi-experimentally designed, 15-year (1993 to 2007) follow-up study was conducted with a total of 13,835 male and 7791 female Japanese workers. They were divided into three groups: participants in the program (1565 males and 742 females), nonparticipant comparative obese controls (1230 males and 605 females), and nonparticipant reference subjects (11,012 males and 6426 females). Hazard ratios were calculated with survival curves drawn to evaluate the mortality effects by the program participation. **Results:** The male participants showed significantly lower mortality risk for all causes of death at hazard ratio = 0.54 (95% confidence interval: 0.31 to 0.94) with significantly different survival curves ($P = 0.014$ by log-rank test) than obese controls. **Conclusions:** The results support a protective effect on mortality by participating in BOOCS program.

For our health and well-being, better lifestyle is undoubtedly important. Many studies have provided scientific evidences showing that healthy behavior, including smoking cessation, physical exercise, low-fat diet, and balanced nutrition, is essential for disease prevention and health promotion. Prevalence of obese workers has increased during these decades, that is, 25.1% for males and 23.9% for females in the United States as a body mass index (BMI) of 30 or higher in 2003 to 2009,[1] and 28.5% for males and 11.6% for females in Japan as a BMI of 25 or higher in 2011.[2] We are now facing to risk of metabolic syndrome especially in developed countries, and the fact shows that substantial proportion of us would improve the ways of our life and health behavior.[3-8]

Key points of health education are logicalness, constructiveness, and persuasiveness for people, those screened as with ill-health condition. Effective and practical health programs should consist of not only an accurate theory but also flexible manner of guidance. Although several practical studies on worksite health programs have been conducted in Japan,[9-13] most of them utilize the traditional approach for lifestyle modification. We have established a new method of health education, Brain-Oriented Obesity Control System (BOOCS), and put it to practice.[14] This is a unique method prioritizing the recovery from fatigue, in particular, "brain fatigue," and it eventually induces better lifestyle modification and improvement of body weight and serum lipids.

From the Ushibuka City Hospital (Dr Hoshuyama), Amakusa, Kumamoto; Department of Medicine and Biosystemic Science (Drs Odashiro and Fukata), Kyushu University Graduate School of Medical Sciences; Faculty of Arts and Science (Dr Maruyama), Kyushu University; and BOOCS Clinic (Dr Saito, Ms Wakana, Ms Fukumitsu, Dr Fujino), Fukuoka, Japan.

Conflicts of interest: None declared.

Address correspondence to: Tsutomu Hoshuyama, MD, Ushibuka City Hospital, 3050 Ushibuka, Amakusa, Kumamoto 863-1901, Japan (goldmedal@hotmail.co.jp).

DOI: 10.1097/JOM.0000000000000399

This study was carried out under a quasi-experimental design, that is, an intervention study without random allocation of subjects with the aim to demonstrate the preventive effect of BOOCS program on mortality during the active employment among the program participants.

MATERIALS AND METHODS

Study Subjects

The all subjects were public service employees working for the municipal governments of Fukuoka Prefecture, Japan. They had the membership of a health service organization that provides a variety of services such as health examinations, health seminars and guidance, and health insurance programs.[15]

Of the members of this health service organization, those who were actively employed as of April 1, 1992, with at least 6 months of employment and aged 59 years or younger as of March 31, 1993, were included in the study population. The newest computerized personnel data file was used to identify the date of his or her employment and establishment of the membership, and the date of his or her retirement (only for the retired).

Definition of Intervention and Reference Group

In 1992, the health service organization introduced the health seminars that were specific to BOOCS program. The seminars were held 10 times a year, which was 1-day or 2-day program and consisted of lectures on health care by physicians and practical exercises by health care professionals such as a physical instructor, a dietician, and a psychologist. All participants received an individual interview of follow-up by occupational health nurses 1 year after the seminar.

At the beginning of the fiscal year 1993 to 1997, the occupational health nurses selected the workers with obesity and the risk of diabetes and/or hypertension with verifying the annual health check-up data of the previous year and sent them a letter to encourage them to participate in the program. The workers without participation histories were selected as priority candidates. The intervention subjects were those who first participated in the program during 1993 to 1997.

For the workers without participation in BOOCS program, conventional health guidance was provided for health promotion and disease prevention. They were divided into two groups as follows. The first group was composed of those with obesity at 25 or higher score of BMI, or with health problems relating to obesity, which was found in the annual health check-up in 1992. They were defined as comparative obese controls. The second group was composed of the rest of the workers after excluding the comparative obese controls, and they were defined as reference subjects.

Characteristics of BOOCS Program

The BOOCS program utilizes psychosomatic approach for behavior modification, which is distinct from the others.[14] Under the two principles and three basic rules (Table 1), effective and active guidance is provided for health promotion and disease prevention. Although lifestyle modification in a conventional approach starts with prohibition and inhibition against unhealthy behaviors such as alcohol drinking, smoking, and high calorie-intake, its strictness frequently results in the rebound of body weight and the appearance

TABLE 1. Two Principles and Three Basic Rules of BOOCS Program[a]

Two principles
1. Do not prohibit or order yourself as possible.
2. Do something pleasant for you.
Three basic rules
1. Do not practice what you dislike, even if it is good for your health.
2. Do not prohibit what you like even if it is bad for your health.
3. Do only what you like among good things and matters for your health.

Abbreviation: BOOCS, Brain-Oriented Obesity Control System.
[a]Adapted from Fujino.[14]

of guilty conscience. On the contrary, the BOOCS program does not induce such dilemmas because it begins with no prohibition and makes us recover from brain fatigue. Moreover, the three basic rules translating the principles easily lead us to modify our behavior for health and well-being in our everyday life.

Follow-Up

All subjects were followed up from April 1, 1993, to March 31, 2008, at longest. The follow-up was stopped when the subject died or retired and lost the membership because of compulsory retirement (usually at the age of 60 years) or voluntary retirement. The follow-up periods for the participants in the program were different according to the year of participation, 1993 to 1997. Personal information, including date of hire and that of retire/death, was computerized and the person years of the active membership were calculated on the basis of the information.

Data Analysis

First, standardized mortality ratios (SMRs) and corresponding 95% confidence intervals (CIs) were calculated. Person years at risk were accumulated for the subjects in the follow-up period. Expected numbers of deaths were calculated by multiplying the person years with sex-, age-, calendar-year-, and cause-specific death rates of the general population in Japan, 1993 to 2007.[16]

Second, hazard ratios (HRs) and corresponding 95% CIs were calculated between participants and comparative obese controls with adjusted by age as of March 31, 1993, and occupation as potential confounders. Also, survival curves were drawn for all deaths between participants and comparative obese controls. Statistical analyses were performed with SAS version 9.3 (SAS Institute Inc, Cary, NC), and PHREG and LIFETIME procedures were used for calculating HRs and drawing survival curves, respectively.

Ethical Issues

This study was approved by the Ethical Review Board of University of Occupational and Environmental Health, Kitakyushu, Japan.

RESULTS

Figure 1 shows a process of recruitment and enrollment of the study subjects. From the personnel files, a total of 21,626 workers (13,835 males and 7791 females) were identified as the study subjects. After excluding 46 of them with no meeting the inclusion criteria, the number of BOOCS participants, comparative obese controls, and reference subjects were 2307 (1565 males and 742 females), 1835 (1230 males and 605 females), and 17,438 (11,012 males and 6426 females), respectively. Mean ages were significantly different among three groups in both males and females. Frequently seen occupations were a clerk and a firefighter in males, and a clerk, a kindergarten teacher/a nurse, and a food supplier in females (Table 2).

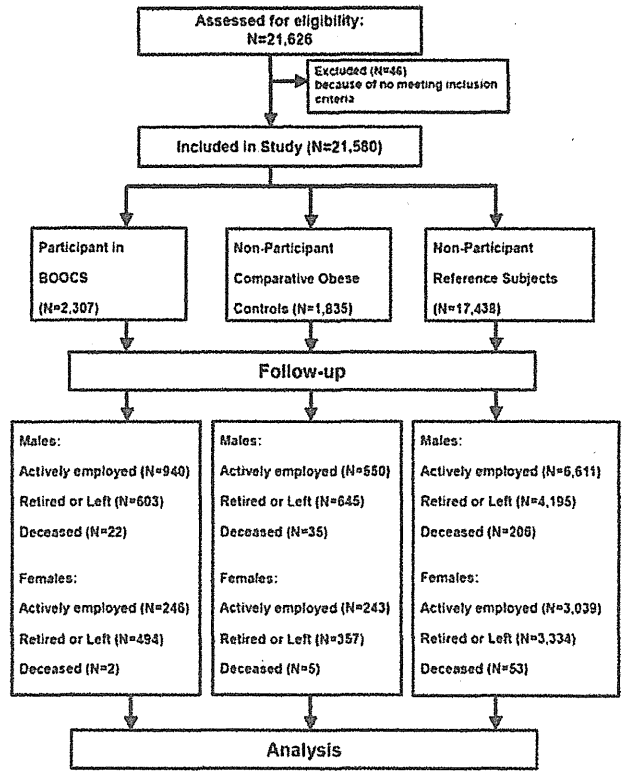

FIGURE 1. Process of recruitment and enrollment in this study.

During the follow-up period, 24 (22 males and 2 females), 40 (35 males and 5 females), and 259 (206 males and 53 females) deceased in participants, comparative obese controls, and reference subjects, respectively (Table 3). In males of the deceased, 10, 16, and 90 persons with malignant neoplasms and 5, 6, and 50 persons with diseases of the circulation were included in the participants, comparative obese controls, and reference subjects, respectively (Table 4).

In males, SMRs for all causes were lower than those of the general population in Japan at 0.36 (95% CI: 0.22 to 0.52) in participants, 0.87 (95% CI: 0.69 to 1.29) in comparative obese controls, and 0.44 (95% CI: 0.38 to 0.51) in reference subjects. For those with malignant neoplasms, decreased SMRs were found to be statistically significant only in participants at 0.48 (95% CI: 0.23 to 0.82) and in reference subjects at 0.57 (95% CI: 0.46 to 0.70). Regarding those deceased because of diseases of the circulation and suicide, no statistically significant decrease or increase in SMRs was seen among both participants and comparative obese controls (Table 4).

In females, despite the lower number of deceased workers, SMRs for all causes were statistically significantly lower among participants at 0.14 (95% CI: 0.01 to 0.41) and among reference subjects at 0.45 (95% CI: 0.33 to 0.58) (Table 4).

Compared with comparative obese controls, HRs for all causes were significantly lower in participants at 0.54 (95% CI: 0.31 to 0.94). Survival curves were also statistically different and such significant mortality changes were persisted during follow-up period ($P = 0.014$ by log-rank test; Fig. 2). Nevertheless, the mortality effect was not found in females with 0.26 (95% CI: 0.02 to 2.52) (data not shown). Regarding other categories of cause of deaths, no significant change was observed in HRs, probably because of the small number of deaths in both males and females (data not shown).